UNIVERSITAT POLITÈCNICA DE CATALUNYA
BARCELONATECH
Escola Superior d'Enginyeries Industrial,
Aeroespacial i Audiovisual de Terrassa

Design project of a low-cost data acquisition system for electromechanical testing of smart materials

BACHELOR FINAL THESIS

Document:
Report

Author:
Laura González Villar

Director /Co-director:
Anastasios Drougkas

Degree:
Bachelor in Industrial Technologies Engineering

Examination session:
Spring, 2023

Abstract

This thesis aims to develop a low-cost data acquisition system to record electrical resistance and deformation data in self-sensing smart cement specimens. Subsequently, the developed system must be tested with cyclic load tests, a text file must be generated with the data obtained and said data must be analysed to extract conclusions about the performance of the system and the piezoresistive "smartness" of the materials.

The most interesting application of this thesis is to implement the system designed in an intelligent cement for Structural Health Monitoring applications, where a structure can be continuously monitored to detect deformations and possible failures before they happen. For this reason, the research on this thesis's state of the art has focused on the current applications of smart cement, current SHM systems and research about low-cost solutions.

To achieve the thesis goals, fluent communication has been established between the thesis director and the author, both by exchanging emails and face-to-face meetings. In addition, face-to-face sessions have been held in the Resistance of Materials laboratory, such as preparing the test specimens and testing the data acquisition system at different points in the thesis.

The results show that the developed system can record electrical resistance and deformation data and generate text files for its processing. The analysis of the obtained data also illustrates the linear relationship between the fractional change in the electrical resistance and the deformation, allowing in this way to characterize the specimens with their gauge factor and thus determine their "smartness".

To sum up, it can be established that this thesis manages to develop a low-cost system for the acquisition of reliable and replicable data and, due to its linear relationship, the cement can be considered "self-sensing" since the application of a load is translated into a change into the electrical resistance, eliminating in this way the need for off-the-shelf strain sensors in SHM systems.

Resum

L'objectiu d'aquesta tesis es elaborar un sistema d'adquisició de dades de baix cost per a captar dades de resistència elèctrica i deformació a provetes de ciment intel·ligent. Posteriorment, el sistema desenvolupat ha de ser testejat amb assajos de carrega cíclica, s'ha de generar un arxiu de text amb les dades obtingudes i s'han d'analitzar les dades per extreure conclusions sobre el funcionament del sistema i l"smartness" piezoresistiva dels materials.

L'aplicació més interesant d'aquesta tesis es implementar el sistema dissenyat en un cement intel·ligent per aplicacions de monitoratge de la salut estructural (Structual Health Monitoring), on l'estat d'una estructura pugui monitorar-se contínuament per detectar deformacions i possibles fallades abans de que passin. Per aquest motiu, la recerca sobre els antecedents de la qüestió d'aquesta tesis s'ha enfocat en les aplicacions actuals que s'estan donant al cement intel·ligent, als sistemes d'SHM actuals i a la recerca de solucions low-cost.

Per tal de aconseguir els objectius proposats, s'ha establert una comunicació fluent entre el director de tesis i l'autora, tant intercanviant correus electrònics com reunions presencials.

Addicionalment, s'han dut a terme sessions presencials al laboratori de Resistència de Materials tan com preparar les provetes com per provar el sistema d'adquisició de dades a diferents punts de la tesis.

Els resultats mostren que el sistema desenvolupat es capaç d'enregistrar dades de resistència elèctrica i deformació i generar arxius de text per al posterior tractament de les dades. L'anàlisi de les dades obtingudes també il·lustra la relació lineal entre el canvi fraccional en la resistència elèctrica i la deformació, permitent d'aquesta manera caracteritzar les provetes amb el seu factor de galga i determinar així la seva "smartness".

A manera de conclusió, es pot establir que aquesta tesis aconsegueix desenvolupar un sistema low-cost per a l'adquisició de dades fiable i replicable i concloure que degut a la seva relació lineal, el cement pot considerar-se "self-sensing" a l'hora de detectar l'aplicació d'una carrega, eliminant així la necessitat de sensors de esforços en sistemes SHM.

Table of contents

Abstract i

Resum i

Table of contents iii

List of tables v

List of figures v

List of abbreviations / Glossary vii

1. Introduction 1

1.1 Object 1

1.2 Scope 1

1.3 Requirements 2

1.4 Justification 3

2 Background and review of the state of the art 7

2.1 Structural health monitoring 7

2.1.1 Phases of SHM 8

2.1.2 DAQ systems for SHM 8

2.1.2.1 Deformation sensors for SHM 9

2.1.2.2 DAQ Devices 11

2.1.3 Low-cost solutions 12

2.2 Applications of self-sensing cement 16

2.2.1 Strain and damage sensing 16

2.2.1.1 Smart high-speed rail infrastructures 18

2.2.1.2 Traffic detection 19

3 Methodology 21

4 Design of the DAQ system 22

4.1 Common components of the DAQ system solution 22

4.1.1 Arduino 22

4.1.2 Strain gauge module 23

4.1.3 Analog to digital converter ADC 25

4.2 Electrical current sensor 27

4.2.1 Development of the electrical current sensor solution and why it couldn't be implemented. 29

4.3 Voltage divider solution 29

5 Development and testing of the DAQ system 31

5.1 Wiring 31

5.2 Code 31

5.3 Excel set-up 32
5.4 Preparation of the cement specimens 36
5.5 Assembly of the strain gauges 38
5.6 Cyclic load tests 41
5.7 Analysis of the recorded data 42
5.7.1 Specimen 1 43
5.7.2 Specimen 3 45
5.7.3 Specimen 4 46
5.7.4 Obtained results summary and interpretation 46
5.8 Using AC vs DC 47

6 Budget summary and/or economic feasibility study 49

7 Analysis and assessment of environmental and social implications 50
7.1 Carbon footprint of cement 50
7.2 Preventive maintenance 51
7.3 Sustainable Development Goals 54

8 Conclusions 57

9 References 58

List of tables

Table 1. Estimated cost (€) of the reference and proposed systems (Source: Design and Validation of a Scalable, Reconfigurable and Low-Cost Structural Health Monitoring System [27]) 13
Table 2. Price comparison of the three systems. (Source: Development of a Low-Cost System for the Accurate Measurement of Structural Vibrations [27]) 14
Table 3. Comparison between the different selected sensors (source: Own.)....24
Table 5. State of the cement specimens (Source: Own)....40
Table 6. Overview of the obtained gauge factors (Source: Own)....47
Table 8. Budget summary (Source: Budget document) 49
Table 9. SDG covered by the thesis (Source: Own) 56

List of figures

Figure 1. Keysight 34461A (Source: Internet [2])....3
Figure 2. Keithley DMM6500 (Source: Internet [3]) 4
Figure 3. DAQ970A (Source: Internet [4]) 4
Figure 4. QuantumX MX840B and MX440B (Internet [5]) 5
Figure 5. CompactDAQ system (Source: Internet [6]) 6
Figure 6. DAQ system scheme (Source: Internet [9])....8
Figure 7. Wheatstone bridge (Source: Internet [12]) 9
Figure 8. Typical Applications of a strain gauge for measurements in screws and bolts (Source: Internet [21])....10
Figure 9. Signal Conditioning for Sensor Measurements (Source: Internet: [20]) 11
Figure 10. 16-Bit versus 24-Bit Resolution (Source: Internet [20])....11
Figure 11. From analogue signal sources to digitalized data ready for processing by computer and software (Source: Internet: [15]) 12
Figure 12. Measurements comparing MADV-DAQ against the commercial DAQ: (a) turbine installation and (b) turbine operation. (Source: MADV-DAQ: Multi-channel Arduino-based differential voltage data acquisition system for remote strain measurement applications [29]) 15
Figure 13. Fractional change in electrical resistance under compressive cyclic loading (Source: Carbon nanotubes and nanofibers as strain and damage sensors for smart cement. [32])....17
Figure 14. Change in electrical resistance under crosshead displacement control three-point bending in a mortar with 0.2 (a) and 0.6% wt. of cement CNF (b). (Source: Carbon nanotubes and nanofibers as strain and damage sensors for smart cement. [32]) 17
Figure 15. SSCCs-engineered smart track slab for high-speed rail monitoring, a schematic of the test site and setup. (Source: In-situ synthesizing carbon nanotubes on cement to develop self-sensing [33]) 18
Figure 16. Potential application of cement-based sensors for traffic vehicle speed monitoring and human motion detection on site. (Source: Potential application of cement-based sensors for traffic vehicle speed monitoring and human motion detection on site. [34])....20
Figure 17.Components of an Arduino UNO board (Source: Internet, [35])....22
Figure 18. Detail of the chosen strain gauge module (Source: Internet, [39] 24
Figure 19.Assembly of the module with an Arduino UNO board (Source, Internet, [39])...25
Figure 20. RDATA Command Sequence (Source: ADS1256 Datasheet [42])....26
Figure 21. Very Low Noise, 24-Bit Analog-to-Digital Converter ADS1256 (Source: Internet [43]) 27

Figure 22.Mounting diagram of the electrical current sensor ACS712 on an Arduino UNO board (Source: Internet, [47]) 28
Figure 23. Voltage divider schematics (Source: Internet [48]) 30
Figure 24. Excel screenshot 1 (Source: Own) 32
Figure 25. Excel screenshot 2 (Source: Own) 32
Figure 26. Excel screenshot 3 (Source: Own) 33
Figure 27. Excel screenshot 4 (Source: Own) 33
Figure 28. Excel screenshot 5 (Source: Own) 33
Figure 29. Excel screenshot 6 (Source: Own) 33
Figure 30. Excel screenshot 7 (Source: Own) 33
Figure 31. Excel screenshot 9 (Source: Own) 34
Figure 32. Excel screenshot 10 (Source: Own) 34
Figure 33. Excel screenshot 11 (Source: Own) 34
Figure 34. Excel screenshot 12 (Source: Own) 35
Figure 35. Excel screenshot 13 (Source: Own) 35
Figure 36. Excel screenshot 14 (Source: Own) 35
Figure 37. Excel screenshot 15 (Source: Own) 36
Figure 38. Excel screenshot 16 (Source: Own) 36
Figure 39. Cement weighing (Source: Own) 37
Figure 40. Cement and water mixing (Source: Own) 37
Figure 41. Molds with marks for the electrodes (Source: Own) 37
Figure 42.Compaction of the cement (Source: Own) 37
Figure 43. Schematic of electromechanical measurement setup for cubic specimens: a) arrangement of embedded mesh electrodes with respect to loading force F. b) Cross section of specimen showing embedded mesh electrode. Dimensions in mm. (Source: Design of a smart lime mortar with conductive micro and nano fillers for structural health monitoring [12]) 37
Figure 44. Electrodes placed on the specimens (Source: Own) 38
Figure 45. Specimens left to dry with a plastic cover (Source: Own) 38
Figure 46. Strain gauges installation set up (Source: Own) 38
Figure 47. Cleaning of the specimens (Source: Own) 39
Figure 48. Installation of a gauge (Source: Own) 39
Figure 49. Elimination of bubbles (Source: Own) 39
Figure 50. Gauges datasheet (Source: Fabricator) 40
Figure 51. Electrical resistance lecture of the installed gauge (Source: Own) 40
Figure 52. Close-up of Specimen 3 (Source: Own) 41
Figure 53. Placement of two wooden pieces between the vice and the specimens (Source: Own) 41
Figure 54. DAQ system set up (Source: Own) 42
Figure 55. V1 vs V2 vs R graph for the third test on Specimen 1 (Source: Own) 43
Figure 56. ΔR/R0 vs ε graph for the third test on Specimen 1 (Source: Own) 44
Figure 57. Dispersion graph ΔR/R0 vs ε for the third test on Specimen 1 (Source: Own) 44
Figure 58. V1 vs V2 vs R graph for the fourth test on Specimen 3 (Source: Own) 45
Figure 59. ΔR/R0 vs ε graph for the fourth test on Specimen 3 (Source: Own) 45
Figure 60. Dispersion graph ΔR/R0 vs ε for the fourth test on Specimen 3 (Source: Own) 46
Figure 61. Specimen's 6 resistance over the time (Source: Own) 48
Figure 62. Actions to a Net Zero future (Source: Internet [62]) 51
Figure 63. Influence of preventive maintenance and corrective maintenance on pavement performance (Source: Automated decision making in highway pavement preventive maintenance based on deep learning [63]) 52
Figure 64. Sustainable development goals (Source: Internet [68]) 54

List of abbreviations / Glossary

ADC: Analog-to-Digital Converter

Arduino: Open hardware board that has an integrated circuit that allows the user to record instructions, connect input and output peripherals and, to sum up, establish a communication between the microcontroller and the computer for diverse applications.

CAN: Controller Area Network. Communication protocol for the transmission of messages in distributed environments. It allows microcontrollers and devices to communicate with each other's applications without a host computer, offering a solution for the management of the communication between multiple CPUs

CNF: Carbon nanofibers

CNT: Carbon nanotubes

CO_{2eq}: Mass of CO_2 that would warm the earth as much as the mass of that gas. It provides a common scale for measuring the climate effects of different gases.

DAQ: Data Acquisition

FPGA: Field-Programmable Gate Array. A programmable integrated circuit that can be configured and reconfigured by the user after manufacturing. It consists of an array of logic elements and programmable interconnects, allowing for the implementation of custom digital circuits.

GCCA: Global Cement and Concrete Association

I^2C: Inter-Integrated Circuit. I^2C is a serial data bus used for communication between different parts of a circuit, for example, between a controller and integrated peripheral circuits. I^2C is beneficial (due to low cost) for peripheral systems that don't need to be fast. It is often used for the transmission of control and configuration data, for example for volume control, analogue-to-digital or digital-to-analogue signal converter with low sample rate, real-time clocks, or small memory spaces.

IoT: Internet of Things. The Internet of Things describes physical objects (or groups of such objects) with sensors, processing ability, software and other technologies that connect and exchange data with other devices and systems over the Internet or other communications networks.

Learn by doing: Educational approach that emphasizes active, hands-on learning experiences as a primary means of acquiring knowledge and skills. It is based on the idea that individuals learn best when they engage in real-world tasks, projects, or activities that require them to actively participate, experiment, and apply what they are learning.

MEMS: (Micro-Electro-Mechanical Systems)

Piezoresistivity: Property of some conductive and semiconductor materials, whose electrical resistance changes when they are subjected to mechanical strain or stress (traction or compression) that deforms them.

SDG: Sustainable Development Goals

SHM: Structural Health Monitoring

SPI: Serial Peripheral Interface. SPI bus is a synchronous serial communication protocol widely used in embedded systems. It enables the exchange of data between a master device and one or more slave devices using four wires: a serial clock (SCK), a master-out-slave-in (MOSI) line for data transmission, a master-in-slave-out (MISO) line for data reception, and a chip select (CS) line for device selection.

SSCC: Self-sensing cementitious composites

True RMS AC voltage: True Root Mean Square AC Voltage. Equivalence of an AC signal to a constant DC value.

Wheatstone bridge: A Wheatstone bridge is an electrical circuit used to measure an unknown electrical resistance by balancing two legs of a bridge circuit, one leg of which includes the unknown component. The primary benefit of the circuit is its ability to provide extremely accurate measurements.

1 Introduction

1.1 Object

This thesis has been planned to design, implement, and test a low-cost data acquisition system based on an Arduino microcontroller board. This microcontroller will be used for the collection of strain and electrical resistivity data generated from a cementitious specimen under mechanical stress and, with posteriority, to determine the smartness of said specimen thanks to its piezoresistive gauge factor. The most interesting application of the development of said DAQ system is to implement it into smart materials structures based on piezoresistivity that could act as a sensor by itself to monitor its state in a continuous way and implement a structural monitoring system.

Arduino is a well-known open hardware microcontroller both for experts and electronics hobbyists. Due to this, there are already Arduino modules to measure electrical current, electrical resistance and strain gauge data. The main goal at the end of this project is to arrange it in an acquisition system, synchronize all data, and connect it with a computer to produce readable text files with all data. [1]

1.2 Scope

The scope that will be treated in this thesis is composed of the following sections:

- **Research about the modules and sensors necessary for the development of the DAQ system:** Investigation about which sensors, modules or any other devices would be necessary for arranging the correct data acquisition system.
- **Familiarization with Arduino.** Learning to program in Arduino language and investigating current solutions of the Arduino usuaries on this issue.
- **Set up the sensors and modules with the Arduino board.** Arrange the sensors and modules with the microcontroller to create the DAQ system.
- **Development of the code for the Arduino microcontroller.** Programming the microcontroller and sensors for capturing the required measurements.
- **Implement the DAQ system.** Integrate the microcontroller with the necessary sensors, modules, a computer, and a specimen and be able to generate a text file with the data acquired by it.
- **Test the system designed on the specimens.** Test if the system captures the electrical resistance and mechanical deformation caused by cyclic load tests and generates a text file.
- **Document the DAQ system.** Once the system is working correctly, document the process, explain the code, and develop connection diagrams since, in that way, anybody could replicate it in their installation.
- **Data analysis.** Process the collected data to generate graphs and extract conclusions.
- **Budget summary.** Is it economically feasible? What is the total cost of this thesis?
- **Conclusions about the developed solution.** Discuss if the developed design is working correctly and if it's a proper option for the problem this thesis tried to resolve.

To perform the testing, the specimens need to be prepared. The scope of this thesis is just to design and implement the DAQ system mentioned previously. For this reason, these specimens will be prepared by a docent from the Department of Resistance of Materials and Structures (even though the author of the thesis will be present on the elaboration, the

decisions about the elaboration of said specimens will be taken by the thesis director and the lab technician).

This thesis is developed with an Arduino microcontroller, which makes impossible the proposition of commercialization of the system.

1.3 Requirements

To perform the thesis, several requirements are needed. Focusing on software tools, the following requirements can be identified:

- **Atenea.** UPC's virtual classroom. Will be used for the disposal of the different thesis documents submitted for evaluation.
- **Google tools such as Gmail and Google Meet.** Used for establishing communication between the thesis director and the alum and following the state of the thesis.
- **Arduino IDE.** For programming the Arduino board.
- **Excel 2021.** For recording and processing the obtained data.
- **Code::Blocks.** For compiling the ADC library used.

Technical requirements are the following:

- **x2 Electrodes for each specimen.** for disposing inside the specimen to connect the electrical current sensor
- **x2 Strain gauges for each specimen.** For measuring the deformation
- **x1 Arduino board.** For processing the collected data
- **x1 Breadboard.** For connecting the sensors with the Arduino board
- **x1 Electrical current sensor.** For capturing electrical current data
- **x1 Electrical resistance.** For developing a voltage divider.
- **x2 Strain gauge modules.** For capturing deformation data
- **x1 High-resolution ADC.** For amplifying electrical current data
- **x6 Specimens made of cement.** To perform the tests on.
- **x1 Power supply.** For the Arduino board
- **x1 Bench vice.** For applying a mechanical load on the specimens

Once the requirements have been met, the experimental part of this thesis can be done. The specifications of this part are the following:

- Administer a voltage of 5V through the Arduino board to the specimens.
- Measure the electrical resistance.
- Measurement of strain data
- At least 1 mechanical deformation measurement, preferably 2 or more
- Synchronize all data and produce data files.

For the testing part of the thesis, only ordinary cement specimens will be tested, which present a limited, but not negligible, amount of piezoresistive smartness. Additionally, applying an AC would be ideal, but an AC power supply wasn't available (For further development on why to use an AC power supply see section *5.8 Using AC vs DC*.) However, the tests can be carried out in the same way as if the specimen used was a smart cementitious material reinforced with micro and nanotubes and the administered current was AC.

1.4 Justification

Nowadays, the current commercial data acquisition systems offer high performance and versatility, but they have a huge inconvenience: a high price.

When we talk about synchronizing the measurements made (either during experimental testing in the lab or from SHM operations in the field) with a computer, the market offers us a huge variety of multimeters that can be connected to a PC to generate a file with all the recorded data.

A few examples for having a big picture of the prices of those multimeters are:

- **Keysight 34461A, from Keysight Technologies.**

This multimeter can measure numerous parameters such as DC voltage, true RMS AC voltage, resistance, frequency and period and temperature, among others, in a huge range of orders of magnitude.

Apart from the multimeter itself, this product also includes its own software tool, BenchVue Software, that allows the user to visualize multiple measurements simultaneously, export measurement data in the desired format (Excel, MATLAB, Microsoft Word…) and monitor and control bench from mobile devices, among other facilities.

To sum up, Keysight 34461A is a high-performance multimeter but, when it comes to its price, it reaches **1.500€** [2]

Figure 1. Keysight 34461A (Source: Internet [2])

- **Keithley DMM6500, from Keithley**

This multimeter includes 15 measurement functions such as capacitance, temperature, and digitizing. Just as Keysight 34461A, it can work on extended ranges, including 10 pA to 10A and 1 mΩ to 100 MΩ.

Additionally, this device also includes its software tool, KickStart Instrument PC Control Software. KickStart allows the user to configure, test, and collect data from multiple instruments and control up to eight instruments at the same time and retrieve millions of readings from each instrument. In addition, it allows exporting data in ready-to-use formats for additional analysis or to share test updates.

Just as the multimeter previously defined, Keithley DMM6500 has a high price, reaching **1.400 €** [3]

Figure 2. Keithley DMM6500 (Source: Internet [3])

Now, it must be taken into consideration also the data acquisition system for strain gauges too. Those systems can cost thousands of euros. For example, this is a data acquisition system from the same fabricant as one of the multimeters above, Keithley:

- **DAQ970A/DAQ973A Data Acquisition System, Keithley**

This data acquisition system measures and converts 14 different input signals such as temperature with thermocouple, frequency and period, DC/AC and capacitance, direct strain and bridge strain among others. It is also able to generate an automatic file copy to a flash drive. As has been mentioned, its price reaches thousands of euros, having a cost of around **2500€** [4]

Figure 3. DAQ970A (Source: Internet [4])

These options, apart from their price, are quite a good solution for lab testing of materials, but in field measurements terms, the most common solutions are modular systems. Those DAQ systems can incorporate multimeters and gauge data readers, capable of being mounted in the field with adequate protection.

Due to the nature of a modular DAQ system, the user has the flexibility to create a solution adequate for his context, being able to add as many modules as he may need. The decision of which modules are included in the DAQ system depends on which data needs to be monitored. The advantage of this system is that you can add/remove modules at any time needed.

Looking into the actual market, different solutions based on modular DAQ systems can be found. One example of this is **QuantumX Modules** from **HBM.** Thanks to those modules, the user can connect the module to the PC, scale several hundred channels in a centralized way or integrate any sensor and transfer its digital value to the CAN or to an analogue voltage output among others. To perform the use of the modules, they must be distributed and installed near to the measurement spots and sensor.

One of the modules of the QuantumX group is the **MX840B universal amplifier**.

This module is compatible with 17 different sensors, such as a strain gauge (full and half-bridge), inductive full and half bridge, piezoresistive full bridge, electric voltage, electric current, ohmic resistance, frequency measurement or rotational speed measurement, that can be connected directly to the 8 channels available.

The frequency of these modules is high, being able to capture 40.000 samples per second on every channel. This acquisition frequency is orders of magnitude higher than what is required for applications in building structures or for the characterization of smart materials.

The price of this module is also a consideration to have in mind. A QuantumX module can reach **10.000€** [5]

Figure 4. QuantumX MX840B and MX440B (Internet [5])

Another remarkable company in the DAQ systems business is National Instruments. NI offers PC-based systems with plug-and-play DAQ devices with fixed functionality or configurable systems that let you mix and match hardware for each different application. Of all the solutions, the focus will be on **CompactDAQ** [6]. This DAQ device has been designed for applications with a wide mix of measurement types, where scalability and flexibility are important.

CompactDAQ is composed by:

A chassis: Allows the device to be connected to a PC through USB or Ethernet. The price of the DAQ chassis can go from **530€ to 3451€** depending on slot count, the operating temperature range, if they have a conformal coating to protect electronics from moisture or if the product supports hardware-based synchronization over the network among other features. [7]

One or more conditioned I/O modules: NI has more than 60 I/O modules for nearly any sensor type that provide signal conditioning and analogue-to-digital. They can be connected to many sensors and buses and support measurements such as temperature, voltage, resistance, and audio frequency, among other features. Defining the price of the modules is a tricky issue since it highly depends on the type of sensors and data that will be recorded. For example, the C Series Relay Output Module has been designed for recording data from motors, actuators, and DC devices. This kind of modules can have a price between 319€ to 1004€ [8]. For other measurements more related to SHM applications, the C Series Universal Analog Input Module could be more adequate. This module includes built-in support for accelerometer, powered sensor, full-bridge, and voltage measurements as well as quarter-bridge, half-bridge, 60 V, and current measurements using measurement-specific adapters. It also can measure signals from sensors such as strain gauges, resistance temperature detectors, thermocouples, load cells, and other powered sensors. Its price can go from **1483€ to 2421€** depending on the maximum sample rate, the

supported sensor type, or the maximum number of differential analogue input channels among others. [9]

A controller: Performs waveform acquisition and software analysis while logging data to onboard or removable SD memory. The price of the controller goes from **5583€ to 9301€** [10] depending on the processor core, slot count, hard drive memory size and the operating temperature range.

Although the recorded data could be analyzed with open-source software such as C# or Python, NI also offers the licenses of application software to quickly log and view data such as LabView, with a price of **2802**€ [11]

Figure 5. CompactDAQ system (Source: Internet [6])

As can be observed, despite NI claims to offer price-competitive solutions on DAQ systems, integrating a NI DAQ system can be priced up to **18000€**, considering that just one module will be needed.

Also, it is necessary to add the price of the sensors themselves and the protection system that will be installed to avoid the module (and the sensors) to suffer damage with the meteorological conditions and other incidents that may occur (these modules are installed near to the sensors to monitor operations in the field). These considerations increase even more the price of a modular system, making it a precise and polyvalent but expensive solution.

As has been seen, the solutions existing on the market offer high performance at a high cost, leaving out the small applications that don't need high frequencies and have a low budget. In addition, for this application, the only interesting data are the electrical resistance and mechanical deformation. Since these modules and multimeters can capture other parameters, this adds an extra cost that wouldn't be needed if we are not interested in measuring a large number of parameters.

The main inconvenience of developing this low-cost DAQ system is that it can only be used for applications that don't require a high frequency, since the maximum frequency that Excel offers (even though the data will be captured by the Arduino microcontroller, it will not be processed by Arduino's software, Arduino IDE, but by Excel to generate text files), is 100 readings per second (100 Hz). Besides that, this is not a deal-breaker for this project since it still can have educational or practical purposes on structural applications that don't need high-frequency data acquisition for its monitoring.

For these reasons this thesis will be developed, to design and test a low-cost data acquisition system for electromechanical testing of smart materials that could be used both at a lab or for SHM operations in the field for applications with data acquisition frequency requirements under 100Hz.

2 Background and review of the state of the art

As has been mentioned in the introduction, this thesis has the goal to design and implement a low-cost data acquisition system for electromechanical testing of smart cementitious materials based on piezoresistivity.

While all cementitious materials exhibit a limited amount of piezoresistive self-sensing capability, Drougkas, A. et al, in their paper, *Design of a smart lime mortar with conductive micro and nano fillers for structural health monitoring* [12], explain that adding electrically conductive micro and nanofillers such as graphite, carbon nanotubes and carbon microfibers provide improved multifunctionality to the matrix material thanks to the improvement of its piezoresistive characteristics. Moreover, it also has a positive impact on the mechanical properties of the cementitious material without compromising its mechanical and chemical compatibility with the original structure.

The necessity of monitoring a structure lies in the implementation of a structural health monitoring system, to assess the performance of buildings. Thanks to these improved piezoresistivity properties, the use of invasive sensors that could cause incompatibilities with the original structure or an impact on the aesthetics of a building (especially on architectural heritage structures) is not needed.

In this chapter, research about existent solutions and applications of the described issue that will be covered by this thesis will be performed.

2.1 Structural health monitoring

Structural health monitoring is the process of observation and analysis of structures, such as bridges, wind energy plants, water, gas and oil pipelines, tunnels, rails, ships, planes, or trains among others to acquire data on their behavior and performance since they are subjected to various internal and external factors that can cause malfunction. Data is collected over time and includes the use of several types of sensors attached to the structure to make this process continuous and automatic.

The main goal of SHM is to detect anomalies in the response of the structure in time to react before serious damage is caused. This system allows to implement maintenance and repair actions in a more efficient way and, due to it, reduces operating costs [13].

The SHM system can transfer the extracted data to an electronic device such as a mobile phone or a computer thanks to IoT technologies and allows to elaborate diagnostics about the safety, strength, and integrity of a structure thanks to the data collected.

As has been said in chapter *2. Background and review of the state of the art*, self-sensing cement can be used to substitute sensors when it comes to measuring resistivity changes in cement mortars. Despite this, it is still difficult to find an actual SHM system that involves smart cement in applications outside academia. In this section, a brief review of the implementation of the phases of implementation of an SHM system and the systems that are being implemented nowadays will be performed.

2.1.1 Phases of SHM

SHM systems can be implemented in a structure with a 4-phase method [14]:

1. **Operational evaluation.**

In this phase, it's necessary to define and identify the damage(s) that are about to be monitored and the conditions that the structure is working under.

2. **Data acquisition, cleansing and normalization.**

In this step, the structure must be fitted with measuring devices. This includes the selection of sensors, in type, number and location to maximize the probability of detection. Moreover, the frequency of inspections (periodic or on-demand after extreme events) must be determined to choose the adequate signal acquisition system and digitalization hardware. After the data has been acquired, it must be cleaned and normalized to dismiss the variations caused by ambient and operational conditions and non-relevant data.

3. **Feature extraction**

Once the data has been treated, damage-related information can be identified. Those features can be physical magnitudes extracted from the structure or statistical signal treatment. In this step, the type and severity of the damage are identified, located, and quantified.

4. **Informed decision making**

With the extracted damage-sensitive characteristics from step 3, numerical and statistical models are applied to identify the current state of the system and, with the help of prediction models, predict the remaining useful life. Based on these predictions, it is possible to perform maintenance actions, extend the lifetime of the structure or program its dismantling based on real data of the structure instead of the intervals defined generically by the fabricator.

2.1.2 DAQ systems for SHM

As has been mentioned previously, one of the most fundamental parts of the implementation of SHM on a structure is the elaboration of a DAQ system. DAQ systems consist of sensors, DAQ modules that provide signal conditioning and data conversion and computing resources including drivers and application software. Those connections can be summarized in Figure 6.

Figure 6. DAQ system scheme (Source: Internet [9])

DAQ systems have the main purpose of acquiring and storing data. Additionally, they should provide real-time and post-recording visualization of the data, since the main goal of installing a DAQ system is to analyze the recorded data. Each system has its necessities but most of the applications looked for in a DAQ system by the engineers can be summarized in data recording, data storing, real-time data visualization, post-recording data review, data analysis using various mathematical and statistical calculations and report generation. [15]

Since this thesis is focused on the design of a low-cost DAQ system for electromechanical testing, the following subsections*, 2.1.2.1 Deformation sensors for SHM* and *2.1.2.2 DAQ Devices*, will be focused on the development of a brief review of the existing commercial solutions for sensors and DAQ modules for recording electromechanical data for SHM.

2.1.2.1 Deformation sensors for SHM

There is a huge variety in which deformation sensors can be found depending on the application that they will perform. This part of the thesis has the purpose of illustrating some of the solutions that a company could choose to implement deformation sensors on its SHM system.

For its simplicity and accuracy, the main products used for measuring deformation values are strain gauges. A strain gauge is a resistor that, installed on a surface, measures the strain of a material or structure at the point where it has been located. When a component is subjected to a force, it causes a deformation that translates into a variation of the nominal resistance of the gauge. This change can be used to determine the force, weight, pressure, tension, compression, torsion, and torque. [16]

The measurements of gauges are based on the concept of a Wheatstone bridge, where a resistance has been replaced for a gauge. In this way, any change in the strain's resistance will unbalance the bridge and produce an output voltage different from 0V.

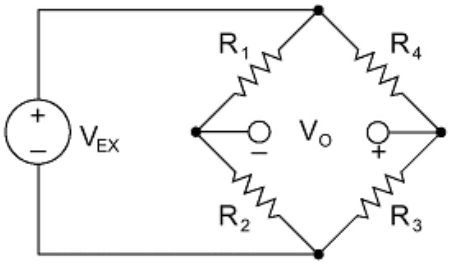

Figure 7. Wheatstone bridge (Source: Internet [12])

Depending on the number of active elements in the Wheatstone bridge, the orientation of the gauges and the type of strain being measured, the configurations of the gauges receive the names quarter (one active strain gauge), half (two active strain gauges), or full bridge (four active strain gauges). [17]

Besides the configuration, it also must be taken into consideration the type of deformation that wants to be recorded. For example, linear strain gauges are preferable for measuring strain across a single plane. Nonetheless, for biaxial stress is preferable to use a rosette foil strain gauge.

The price of the pack of 10 linear gauges changes depending on the supplier, for example, HBM sells it for **209.95€**, and RS for **215.82€**

Based on the strain gauge performance, other sensors for more specific applications have been developed. Some examples of those deformation sensors for SHM are:

Vibrating Wire Strain Gauges [18] [19] [20]

Those sensors can be implemented by arc or spot welding on steel structures and/or be embedded into concrete structures. Each gauge consists of two blocks with a tensioned steel wire between them. The deformations applied on the structure manifest on the gauge as a change in the tension in the wire that will modify the resonant frequency of the wire because of the relative movement between the blocks. Their frequency output is immune to electrical noise, can tolerate wet wiring and are capable of signal transmission over several kilometres. Vibrating wire strain gauges are implanted in several structures such as concrete dams, bridges, tunnels, or roadways among others. The price of these sensors depends on the supplier, but most of them are between **80 to 130€/unit.**

Strain gauges for measurements in screws and bolts [21] [22]

These sensors are used for measuring the tensile strain of a bolt, being inserted into a pre-drilled hole in the bolt. They're useful for measuring tensions in a bolt when an ordinary strain gauge cannot be installed on the bolt surface.

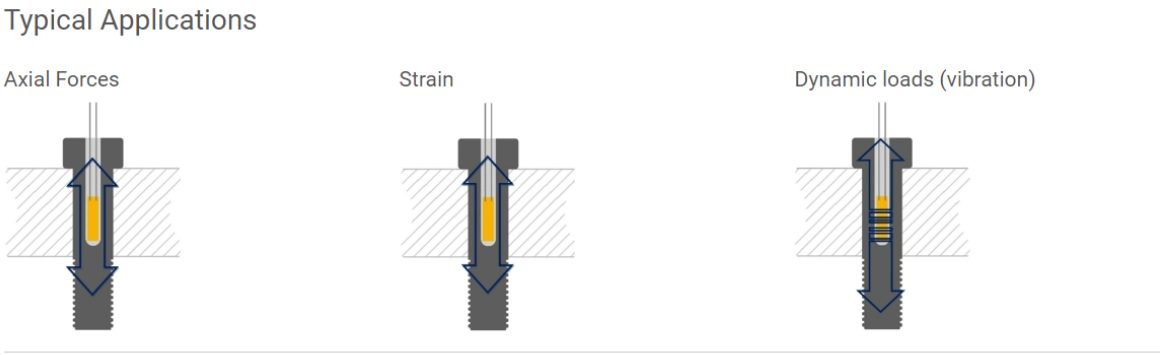

Figure 8. Typical Applications of a strain gauge for measurements in screws and bolts (Source: Internet [21])

HBM company offers this sensor for a price between **223 and 226€/5 units.**

Strain Gauges for Residual Stress Analysis [23] [24]

Residual stress is a type of tension/stress that remains in a material after the cause that produces it has already stopped. Those sensors are used for determining residual stresses in processes such as casting, welding, and forming by drilling a small hole in the center of the strain gauge. This hole will remove material that will release the stress and measure the relaxed residual stress in the vicinity of the hole. Omega company offers this sensor for a price of **221€/5 units** and HBM offers them for **241€/5 units.**

It must be considered that the number of gauges or sensors used for SHM must be dimensioned according to the structure that will be monitored, meaning that the prices of the sensors will be multiplied.

2.1.2.2 DAQ Devices

As has been mentioned in subsection *2.1.2 DAQ systems for SHM*, a DAQ system does not only consist of the sensors but also of a hardware system: the DAQ device.

DAQ devices have two main responsibilities: signal conditioning and analogue-to-digital conversion.

Signal conditioning is the process of taking analogue outputs from the sensors and preparing them to be sampled digitally. Each sensor has different needs when it comes to signal conditioning. Most of the signals have the common necessity to linearize the output. Others may need amplification to a nominal level, isolation from the noise or filtering. Each signal conditioning circuitry must be designed to perform the elemental normalizing of the sensor output and prepare it for digitizing having into consideration the particularities of each measurement. Since every sensor type is different, the signal conditioners must conform perfectly to them. [15] [25]

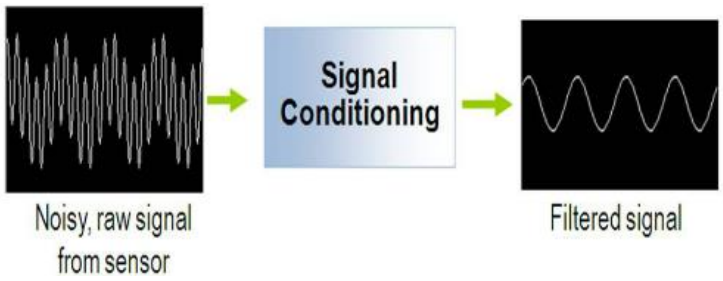

Figure 9. Signal Conditioning for Sensor Measurements (Source: Internet: [20])

An ADC takes an analogue signal and converts it into a binary number, and thanks to this, each binary number can represent a certain voltage level. Once the signal has been transformed into a digital value, it can be processed and analyzed by a software to extract conclusions about the element that is being monitored. Depending on the number of binary levels that an ADC can use to represent a signal, it will have a higher or lower resolution. Figure 10 shows a comparation between the resolution of a 12-bit, 16-bit and 24-bit ADC.

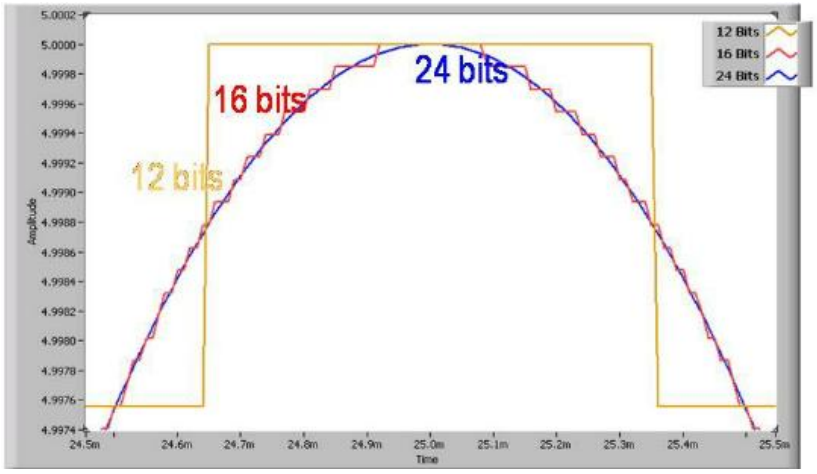

Figure 10. 16-Bit versus 24-Bit Resolution (Source: Internet [20])

The process described before can be summarized in Figure 11:

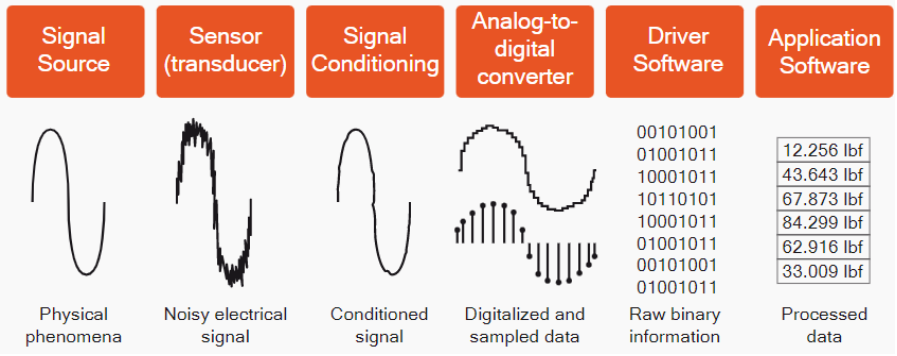

Figure 11. From analogue signal sources to digitalized data ready for processing by computer and software (Source: Internet: [15])

The selected solution for a DAQ device will depend on many parameters such as the kind of signals that need to be measured/generated, the frequency of acquiring/generating samples of the signal or the resolution or the maximum error allowed [26]. Those range of capabilities and specifications make the prices of DAQ devices fluctuate. Dewesoft [19] estimated the price per channel (each channel allows to record d different kinds of data from different sensors using the same DAQ module) as follows:

- Low-end DAQ systems: **$200 - 500 per channel**
- Mid-range DAQ systems: **$500-1000 per channel**
- High-end DAQ systems: **$1000-2000 per channel**

Section *1.4 Justification* shows the high prices that DAQ modules can reach. Those high prices make the implementation of a DAQ system for SHM unaffordable for low-budget projects or companies. This leads this thesis to subsection 2.1.3*: Low-cost solutions.*

2.1.3 Low-cost solutions

Due to the high costs that the implementation of an SHM system represents, low-cost SHM systems have been studied by several researchers. Despite that, there isn't any commercial solution to this issue currently. Therefore, this subsection will be focused on a review of the solutions that some authors have proposed in their respective papers.

In their paper, *Design and Validation of a Scalable, Reconfigurable and Low-Cost Structural Health Monitoring System* [27], Villacorta, J. J. et al. designed, developed and tested a low-cost SHM system based on MEMS (Micro-Electro-Mechanic Systems) triaxial accelerometers. The control system was based on myRIO, a real-time embedded evaluation board developed by National Instruments which incorporates an FPGA that can be programmed using the LabVIEW graphical programing language. The main goal of the authors was to develop a low-cost SHM system based on the use of wireless networks to monitor buildings, together with the use of MEMS accelerometers.

The sensors used by the researchers were ADXL355 accelerometers. Those sensors allow the measurement of vibrations with high resolution and very low noise and can be configurated to create a wireless sensor network. The low noise performance of the

ADXL355 series with low power consumption allows its use on low-level vibration measurement applications, such as SHM, at an affordable cost.

The myRIO units allow to connect of up to 6 sensors each. Those devices are the ones in charge to carry out the synchronous acquisition of data from the attached ADXL355 sensors and are governed by a PC that manages the myRIO platforms connected to the system using a Wi-Fi interface. The PC sends the configuration of the six accelerometer sensors attached to the myRIO device, controls when the acquisition starts and when it stops, and receives the acquired data from the accelerometers for further processing.

After developing the SHM system, the investigators validated it by comparing the data measured by their set-up with a conventional SHM system based on piezoelectric accelerometers. The tests were performed on a wood beam excited with an electromechanical shaker.

The tests showed a high correlation in the behavior of both systems, being possible to conclude that the proposed system was sufficiently accurate and sensitive for operative purposes, with the added value of being significantly more affordable compared to other commercial solutions. In Table 1 the difference in prices between the commercial system and the low-cost system of the authors can be appreciated.

Element	Reference System			Proposed System		
	Model	Cost/Unit	Total	Model	Cost/Unit	Total
DAQ	DS-SIRIUS	6500	6500	myRIO 1900	580	580
6× Accelerometers	KS76C.100	350	2100	ADXL355 + Box	50	300
Cables	UNF to BNC	75	450	RJ45 to RJ45	8	48
Total cost			9050			928

Table 1. Estimated cost (€) of the reference and proposed systems (Source: Design and Validation of a Scalable, Reconfigurable and Low-Cost Structural Health Monitoring System [27])

As can be observed, the low-cost system is 10 times cheaper than the reference one, being a more affordable option for vibration tests used to measure the structural response and provide clues about the existence of some type of structural damage.

Other investigators that have tried to offer a low-cost solution for SHM are Komarizadehasl, S. et al. Their paper, *Development of a Low-Cost System for the Accurate Measurement of Structural Vibrations* [28], is focused on the design of a Cost Hyper-Efficient Arduino Product (CHEAP) since the DAQ systems existing nowadays for recording the vibration of structures have a high cost, which limits its use to structures with a relatively high structural health monitoring budget.

The dispositive designed by the researchers, CHEAP, is composed of three elements:

1. Microcontroller: The microcontroller used in this project was an Arduino Due, since it can provide a reasonable amount of memory to upload complicated codes and has a faster clock speed (84 MHz) of communication compared with other alternatives.
2. Accelerometers: Five low-cost accelerometers that are connected to an Arduino microcontroller as their data acquisition system. The sensors chosen for this project were the MPU9250 since they have a reasonable price (5.76€), use less energy, have less noise density, and have a better range of frequency (especially on low-frequency signals) in comparison with other low-cost solutions.

3. Multiplexor: The sensors communicate with the Arduino thanks to an I^2C protocol (conformed by multiple slave digital integrated circuits (Sensors) and a master chips (Arduino)). The Arduino needs a different address for each connected component to its I^2C port to interact and control the sensor. Thanks to a multiplexor, in this case, the TCA9548A, Arduino can change the address and select different sensors. The price of this multiplexor was 3.22€

Once recorded by Arduino, the data is saved into a PC using Python.

After designing CHEAP, it was tested and compared with two piezoelectric sensors (393A03, a uniaxial piezoelectric accelerometer, and 356B18, a triaxial piezoelectric accelerometer) with low noise densities connected to a DAQ system with 12 channels for reporting separated readings. The tests, consisting of the application of dynamic movements with low-range amplitudes and frequencies ranging from 0.5 to 10Hz, had the goal of comparing the accuracy, resolution, and error of CHEAP with traditional expensive sensors.

The tests shown that all the accelerometers work correctly on frequencies equal to or higher than 2 Hz and report the input frequencies precisely. Moreover, CHEP was able to capture low frequencies, while the traditional sensors were unable to read accurately frequencies lower than 2 Hz with low acceleration amplitudes.

Focusing on the prices, Table 2 summarizes the cost of each system.

System	Cost of the Accelerometer (€)	Cost of the Microcontroller (€)	Cost of the Cable (€)	Cost Real-Time Controller (€)	Cost Vibration Input Module (€)	Dimension of the Sensing Part (mm)	Weight of the Sensing Part (gr)
393A03	710	-	75	2010	2050	28 × 28 × 56	210
356B18	1300	-	210	2010	2050	20 × 26 × 20	25
CHEAP	36.1	38.017	10	-	-	50 × 50 × 10	357

Table 2. Price comparison of the three systems. (Source: Development of a Low-Cost System for the Accurate Measurement of Structural Vibrations [27])

As can be observed, the price of an acquisition system with a single 393A03 is 57 times higher than CHEAP. Besides the prices observed in Table 2, to make a fair price comparison between the control systems and CHEAP, the full capacity of the equipment should be considered since real-time control provides 12 channels, and the vibration module has four channels. Working at full capacity, 12 393A03 accelerometers, 12 sets of single channeled cables and one real-time controller and three vibration input modules are needed, leading to a price of 17,580 €. In the 356B18 scenario, 4 sensors, 4 sets of three channeled cables, one real-time controller and three vibration input modules would be needed, and its price would be up to 14,200€. Using 12 sets of CHEAP, it can be configured to make a triaxial sensor that can perform as 12 uniaxial accelerometers or 4 triaxial accelerometers with a proximate price of 1008.84€.

The researchers conclude that its proposal, CHEAP, works better on low frequency and low amplitude accelerations compared with 393A03 and has a price 17 times lower than the usual solutions. Komarizadehasl, S. et al. explain that it could be useful for structural health monitoring of structures with a low budget or with low frequencies.

Both examples, from Villacorta, J. J. et al. and from Komarizadehasl, S. et al., are focused on piezoelectrical accelerometers. When it comes to low-cost SHM solutions with strain gauges based on piezoresistivity, the literature reduces significantly. The most relevant paper about the discussed issue is *MADV-DAQ: Multi-channel Arduino-based differential voltage data acquisition system for remote strain measurement applications* [29] from Louw,

H. et al. While other Arduino forums or papers such as *A study of strain and deformation measurement using the Arduino microcontroller and strain gauges devices* [30], from Silva, A. L. et al., are only focused on the designing of a DAQ system with a strain gauge module and an Arduino microcontroller for academical purposes, the work from Louw, H. et al. come up with an actual SHM application of said DAQ system.

In their paper, *MADV-DAQ: Multi-channel Arduino-based differential voltage data acquisition system for remote strain measurement applications,* the authors develop, test, fabricate, install, and validate a low-cost, multi-channel, Arduino-based differential voltage DAQ of multiple remote and battery-powered Wheatstone bridge-based strain sensors for wind turbines. Said tests were developed in a wind turbine from an onshore wind farm in South Africa.

Said DAQ system was designed to implement IoT technologies to be able to control the DAQ remotely over the internet and integrate measurements with existing data platforms. The proposed system had to perform a continuous and autonomous operation over two years with a backup power supply for a continuous, 7-day operational period.

The Arduino microcontroller works as the primary DAQ system. Additionally, a secondary Raspberry Pi relays the information to two independent data platforms for long-term storage and analysis and, in case of failure, Arduino stores data on an SD card. To provide more accurate readings, a low-cost, high-resolution analogue-to-digital converter is implemented in the author's design.

After developing their DAQ system, it was implemented on the wind turbine mentioned previously, which was monitored both during foundation construction and turbine installation and after turbine commissioning. Besides the MADV-DAQ system, the researchers also installed a commercial DAQ system.

As can be observed in Figure 12, both measurements were generally in sync.

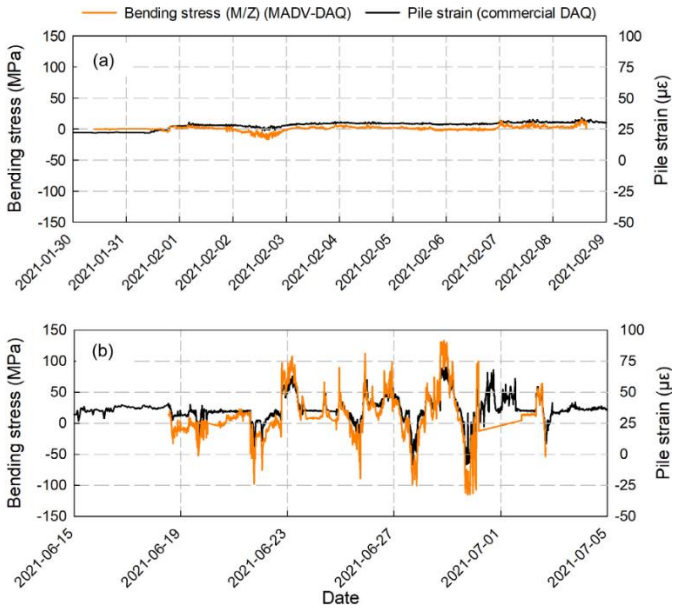

Figure 12. Measurements comparing MADV-DAQ against the commercial DAQ: (a) turbine installation and (b) turbine operation. (Source: MADV-DAQ: Multi-channel Arduino-based differential voltage data acquisition system for remote strain measurement applications [29])

Finally, Louw, H. et al. proved that their system provides reliable strain measures related to a wind tower and can quantify the true magnitude of the loads that are being transferred to the foundation. Moreover, MADV-DAQ can be used as a universal data acquisition system, compatible with any Wheatstone bridge-based sensor design, including strain gauges, tensiometers and similar MEMS-based sensors.

To summarize, low-cost solutions, even if they have been investigated, are still not a reality. Their performance, as the papers show, can be compared to the performance of traditional, more expensive, solutions. The commercialization of those low-cost solutions could bring the opportunity to implement SHM on not just structural elements that will cause both human and economical considerable losses in case of failures such as bridges or energy plants, as has been mentioned before, but also in other not-so-crucial structures such as buildings, improving its lifetime and reducing its carbon footprint (this issue will be discussed in chapter *7. Analysis and assessment of environmental and social implications*).

It also must be considered that this thesis is not just focused on the design of a DAQ system but also on the consideration that the most interesting application of that said DAQ system will be the implementation onto a smart cementitious material that could act as a sensor by itself. The following section, *2.2 Applications of self-sensing cement*, will be focused on reviewing the state of the art of implementation of smart materials in SHM.

2.2 Applications of self-sensing cement

As has been previously mentioned, the use of a smart cement mortar based on piezoresistivity is a field of huge interest since it implies that a structure can be used as a sensor for monitoring its health and behavior. This kind of cementitious material is known as self-sensing.

Self-sensing cement and concretes have been investigated by many authors in their respective papers. In this chapter, a brief review of the added value that the self-sensing cement represents in front of the regular one will be performed, as well as some examples of its applications.

2.2.1 Strain and damage sensing

All the applications of the self-sensing cement start from the same premise: Its capacity of detecting strain and damage thanks to its piezoresistive properties. Those properties imply that when a mechanical strain is applied, a change in the electrical resistivity is produced. In the work of Drougkas, A. et al. [12], the authors explain that the gauge factor λ of a self-sensing cement is an indicator of said piezoresistive effect during mechanical loading. A higher gauge factor indicates higher sensitivity of the material's electrical resistivity to applied strain.

Many researchers have investigated this propriety coming out with very remarkable results. In this chapter, the focus will be put on a paper from Dalla, P. et al*., Carbon nanotubes and nanofibers as strain and damage sensors for smart cement* [32]. The authors of said paper reported the strain and damage sensing potential of cement mortar with embedded carbon nanotubes and carbon nanofibers. The specimens were submitted to various tests to determine the material's surface electrical resistivity, its piezoresistive response under cyclic compressive loading and its ability for damage detection under pure bending.

On one hand, the researchers prepared the specimens with a CNT concentration of 0.6% by weight of cement in the mortars. Moreover, in the production phase, metallic grids were embedded in them to measure the electrical resistivity simultaneously in four points. In response to the cyclic compression tests, the mortars exhibited remarkable piezoresistive characteristics with fully recoverable electrical resistances at the end of each cycle. The electrical resistance varied in an inversely proportional way regarding the applied stress due to the instant compaction level.

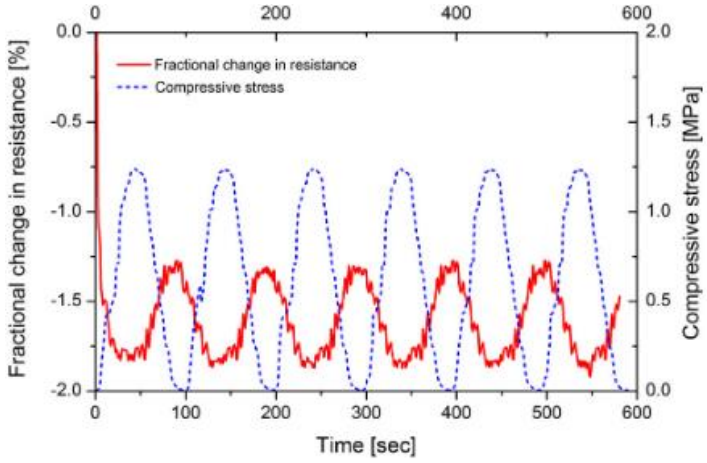

Figure 13. Fractional change in electrical resistance under compressive cyclic loading (Source: Carbon nanotubes and nanofibers as strain and damage sensors for smart cement. [32])

On the other hand, essays with carbon nanofibers were performed, comparing the performance of a concentration of 0.2% and 0.6% of CNF by weight of cement in the mortars. The three-point bending tests on the mortar with 0.2% of CNF showed the remarkable damage-sensing capability of embedded nano-inclusions on cement mortars. This phenomenon was reflected in dramatic resistivity jumps when the maximum load was achieved. This sensing capability in early-stage of the three-point bending tests provides valuable warning signs and considerable time for reaction.

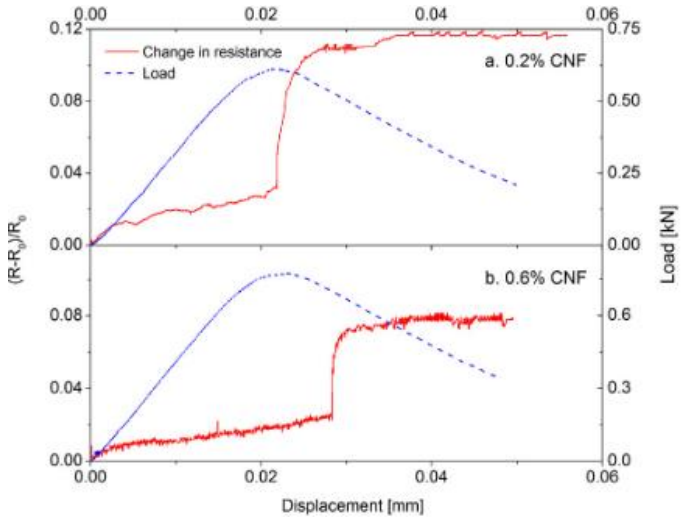

Figure 14. Change in electrical resistance under crosshead displacement control three-point bending in a mortar with 0.2 (a) and 0.6% wt. of cement CNF (b). (Source: Carbon nanotubes and nanofibers as strain and damage sensors for smart cement. [32])

These properties of smart self-sensing cement can be applied in plenty of fields such as concrete railway ties on long-line railroads, transit lines, hospital operating room floors and cathodic protection systems. All these applications are based on the fact that, in smart cement, the tubes can act as internal self-monitoring sensors for inner defects detection, eliminating the need for embedded, attached, or remote sensing systems.

In the following subsections, a couple of examples of self-sensing cement applications developed by several investigators will be developed.

2.2.1.1 Smart high-speed rail infrastructures

In their paper, *In-situ synthesizing carbon nanotubes on cement to develop self-sensing cementitious composites for smart high-speed rail infrastructures* [33], the authors Ding, S. et al., develop a system able to synthesize carbon nanotubes on cement in-situ, to mitigate the dispersion, since the carbon nanotubes performance, manufacturing and application are limited by the uniform dispersion of them inside the cement, and improve their efficiency.

The motivation of the authors was to ensure the safety of rail transportation offering a long-term, wide distribution, and low-cost monitoring system for high-speed rail structures. For achieving this goal, the researchers developed self-sensing cementitious composites engineered smart track slabs for axle counting and speed detection.

After developing their own cement with carbon nanotubes, *CNT@Cem*, the authors applied it on a real high-speed railway line (Shanghai-Hangzhou High-speed Railway, K005, China), and set it up as Figure 15 shows:

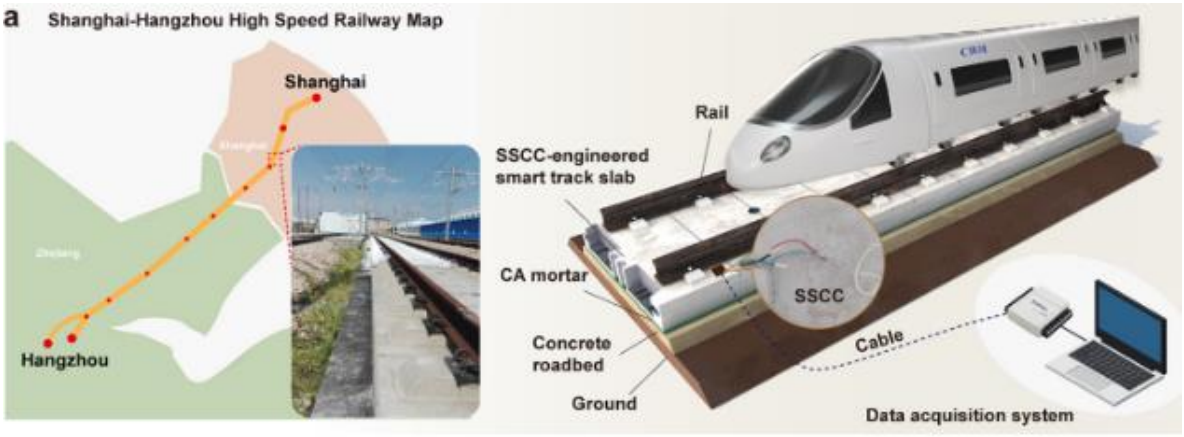

Figure 15. SSCCs-engineered smart track slab for high-speed rail monitoring, a schematic of the test site and setup. (Source: In-situ synthesizing carbon nanotubes on cement to develop self-sensing [33])

Thanks to this setup, the DAQ system could detect the train that was circulating at the moment, since the 8-car generated 8 sharp peaks of voltage change in the trace that was being recorded and, the 16-car generated 16 peaks. Once the train type has been identified, and knowing the distances between bogie centers, the instantaneous and average train speeds can be obtained. Furthermore, comparing the first car's instantaneous speed and the last car's instantaneous speed, the acceleration of the whole train can be calculated.

Additionally, the investigators found that the peak amplitude corresponding to each bogie was different due to the different weights of each car. In this way, excessive load that causes degradation in the trains and the railway infrastructure can be detected and corrected.

Finally, the authors concluded that CNT@Cem demonstrated repeatability, stability, adaptability to various applied conditions and fast response and recovery, meaning that it could be applied in long-term and real-time high-speed railway infrastructure monitoring.

2.2.1.2 Traffic detection

This chapter will be based on the paper *Application of intrinsic self-sensing cement-based sensor for traffic detection of human motion and vehicle speed* [34], by Dong, W. et al., where the authors developed a smart concrete pavement for intelligent infrastructure thanks to a self-sensing smart pavement with embedded cement-based sensors.

With their work, the authors intended to offer an alternative to current monitoring techniques such as video surveillance and infrared speed detector for detecting traffic flow, running speed or truckload. Those solutions can have a high cost, low durability, low efficiency, non-real-time observation, and low degree of automation.

To create the smart pavement, the researchers embedded the multiple precast cement-based sensors (the enhanced piezoresistivity of cement-based sensors was achieved by adopting carbon nanofiber) connected in series into a small-scaled mortar slab to increase the sensing range. Afterwards, to the performance of the mortar slab, it was tested with three different loading patterns applied through experimental cyclic compression simulating human weight in different motions, and the simulated traffic load at multiple speeds.

The results showed that the smart pavement exhibited linear and repeatable fractional changes of resistivity in response to cyclic compression force and was able to monitor human motions such as 'up-down' feet or jumping movements. This monitoring of human movements could be useful in security and accident prevention applications since it can be used for people counting, crowd flow monitoring, housing security, and even body weighing.

When it comes to vehicles, the mortar slab was able to detect the exact vehicle speed with high accuracy for car speeds up to 40 km/h (the authors explain that, for detect high-speed vehicles, the advanced data acquisition system with a higher data collection rate should be applied), being a useful tool for monitoring the traffic flow, speed and even weigh-in-motion.

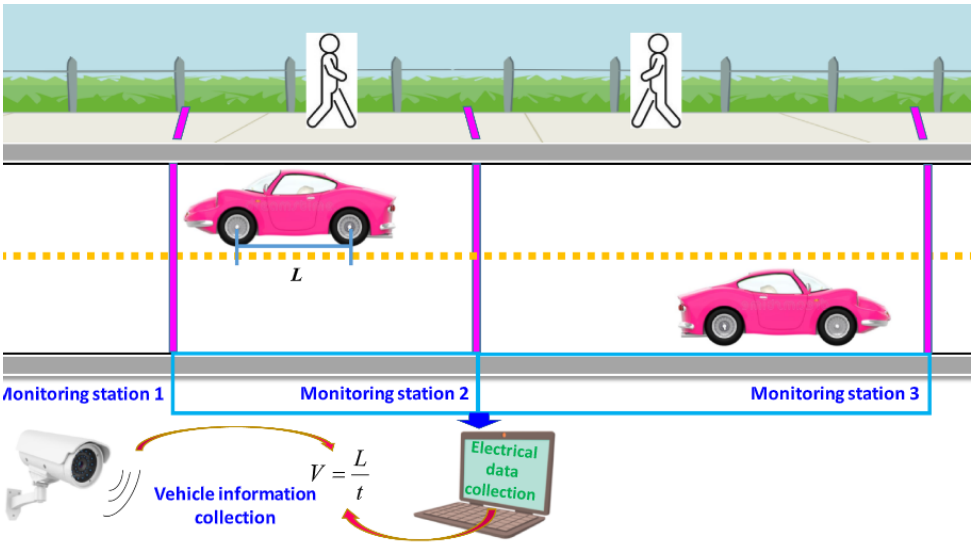

Figure 16. Potential application of cement-based sensors for traffic vehicle speed monitoring and human motion detection on site. (Source: Potential application of cement-based sensors for traffic vehicle speed monitoring and human motion detection on site. [34])

It is hard to find a paper where the two concepts, self-sensing cement and low-cost DAQ system, get linked. Due to this, this thesis will be developed, since those two fields fed one another. Since the strain will be translated into a change in the electrical resistance (in this thesis thanks to the electrodes that the cement specimen contains, since they will get closer one to another when a load is applied, reducing the electrical resistance between them.) strain sensors will no longer be needed, contributing to making the system cost-effective.

3 Methodology

To cover the scope of this thesis, it's important to define a methodology. Due to this, in this chapter, a list of the steps to follow to accomplish the goals of the thesis will be elaborated.

1. **Establish fluent communication between the thesis director and the student.** In this case, the channel chosen has been Gmail.
2. **Definition of the problem and goals.** Since this thesis is based on previous research of the thesis director, the problem and the goals were described since the beginning of the investigation.
3. **Perform a bibliographic review.** This review had to be done not just to acknowledge which solutions on the field were being implemented nowadays (for further development on this issue see chapter *2. Background and review of the state of the art*) but also because, as has been mentioned with priority on this thesis, due to the open-source nature of Arduino, it has a very extensive community that documents their projects on different platforms such as GitHub or the official Arduino forum, which can be a good starting point to the development of the thesis solution.
4. **Design the DAQ system.** Connect the sensors and modules to the Arduino microcontroller and develop the code for recording deformation and electrical resistance data.
5. **Test the DAQ system and fix it if necessary.** Check if the DAQ system is working correctly and perform the necessary corrections.
6. **Implementation of the DAQ system and cyclic load tests.** Implement the DAQ system in the cementitious specimens and perform cyclic load tests while recording data and generating text files with it.
7. **Analysis and conclusions.** Process the data, discuss the results of the tests with the thesis director and extract conclusions.

Overall, the development of this thesis was based on the learn-by-doing educational approach, where the acquisition of knowledge about how to program and wire the DAQ system took place as it was being performed.

The necessary tools to accomplish this methodology can be found in section *1.3 Requirements*.

4 Design of the DAQ system

The main goal of this thesis is to design and implement a low-cost data acquisition system for electromechanical testing of smart materials based on an Arduino microcontroller. To record electrical resistance data, two options were considered:

1. Record electrical current data and then, knowing the applied voltage and with Ohm's Law, calculate the electrical resistance.

2. With an additional known resistance, set up a voltage divider.

Both options share common components. For that reason, this chapter will be divided into a review of said components, the particularities of the option selected in the first place, the development of said option and why it didn't work out and the particularities of the second and final option. (For the development of the final solution see chapter *5. Development and testing of the DAQ system*)

4.1 Common components of the DAQ system solution

4.1.1 Arduino

The central device of this project is an Arduino board. As has been mentioned in the object section of this thesis, Arduino is an open hardware board that has an integrated circuit that allows the user to record instructions, connect input and output peripherals and establish communication between the microcontroller and the computer for several diverse applications.

Arduino offers different models of boards. Some of them are more generalist and others are designed for specific applications. Most of these boards share the common components that can be observed in Figure 17:

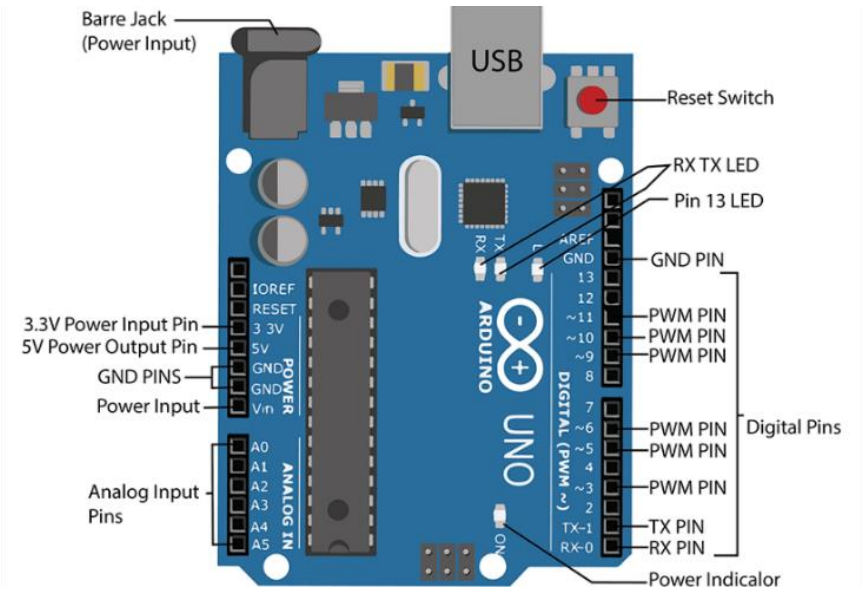

Figure 17.Components of an Arduino UNO board (Source: Internet, [35])

A **barre jack**, **power input pin** and a **USB connection**, to connect the board to a power source in different ways.

A series of **pins** for connecting wires to develop the chosen application of the board. Arduino contains the following pins [35]:

- **Ground or GND** to ground the circuit.
- **5V** to provide 5V to the circuits.
- **Analog Pins** for reading analogue voltage values from sensors and converting them into digital values.
- **Digital Pins** for digital inputs and outputs. The 13th pin is linked to **Pin 13 LED,** which will light up when the pin is in a high state (when its value is equal to 1)
- **PWM Pins**, digital pins that can also be used for pulse-width modulation.
- **RX – TX** used to establish serial communication with other Arduino boards or computers. Those pins have associated **RX – TX LEDs** that light up whenever the Arduino board is receiving or transmitting data on these pins.

It also contains a **reset button** for restarting the code and a **power indicator LED** that lights up when the board is connected to a power source.

As has been mentioned with anteriority, Arduino offers boards with extra specifications. Some examples of those boards are [36]:

- **ARDUINO UNO WiFi REV2.** For IoT applications such as building a sensor network connected to a router or connecting any device to a WiFi network. It has a price of **46,70€**
- **Arduino MKR Vidor 4000.** Able to work with FPGAs, allowing to create of a board where all pins are PWM signals or capture sound in real-time among other applications. It allows the connection to the IoT Cloud, and it is also adequate for high-speed computation. Its price is **75,50€**
- **Portenta H7.** This model is an Arduino IoT Cloud-compatible board, it also simultaneously runs high-level code along with real-time tasks. The design includes two processors that can run tasks in parallel. Its price is **99,00€**

With these examples can be observed that Arduino also offers specific applications and high-technology solutions, but this causes an increment in the prices. For the application that is about to be developed in this thesis, there are no special requirements that couldn't be met. The use of a more specific board will only increase the price of the solution.

This leads us to choose **Arduino UNO Rev3**. The Uno board is the first in a series of USB Arduino boards, and the reference model for the Arduino platform. This board is the most used and documented board of the whole Arduino family, which will facilitate the development of the solution. Its price is **24,00€**, significantly more affordable than the other boards.

4.1.2 Strain gauge module

Deformation will be measured thanks to two strain gauges in a quarter-bridge configuration. As has been explained in subsection *2.1.2.1 Deformation sensors for SHM* of this thesis, when there is no load acting, the output voltage of the Wheatstone bridge is equal to zero. When a force is applied and, in consequence, the material is deformed, the strain gauge varies its resistance, as it deforms with the material, causing a variation in the output voltage.

Strain gauges have a huge capacity of detecting changes in the electrical resistance of their wires. Any small deformation causes a change in the output voltage. Despite that, the signal output is very low, and cannot be measured by Arduino properly. Due to this, the utilization of gauges needs to be complemented with a signal amplifier to determine changes with accuracy.

Strain gauge modules detect the strain, and thanks to the amplifier and potentiometer that the board contains, those readings can be passed to a microcontroller to obtain the mentioned data. [37] [38]

Nowadays, most of the available gauge modules are compatible with Arduino UNO. In this chapter, a comparison between three modules, **HCSENS0036** [39], **SEN77631Y3** [40] and **CT0070SGS** [41] will be performed, and a final model for the DAQ system will be chosen.

	HCSENS0036	SEN77631Y3	CT0070SGS
Compatible with Arduino?	Yes	Yes	Yes
Working Voltage	5V	5V	5V
Output Voltage	0 - 3.5V	0 - 3.5V	0 - 3.5V
Dimension	32mm X 17mm	32mm X 17mm	32mm X 17mm
Sensor type	BF350-3AA	BF350-3AA	BF350-3AA

Table 3. Comparison between the different selected sensors (source: Own.)

The price depends on the chosen suppliers, but none of the modules above has a higher price than **12€**.

As can be observed, the utilization of strain gauge modules for Arduino is a normalized application and, due to this, all the modules present predetermined characteristics. This implies that the selection of one or another module will not influence the project.

The final chosen module will be **HCSENS0036** since it is the module that presents more information about its assembly with an Arduino board.

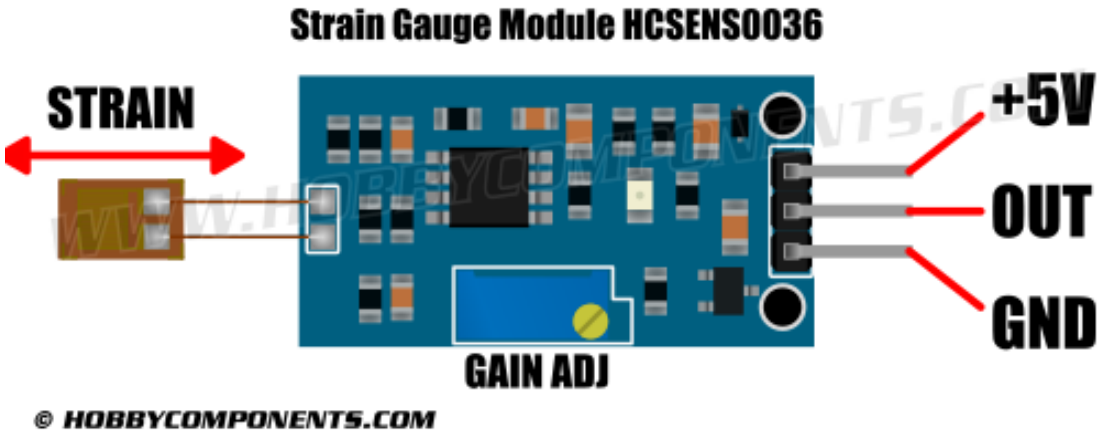

Figure 18. Detail of the chosen strain gauge module (Source: Internet, [39]

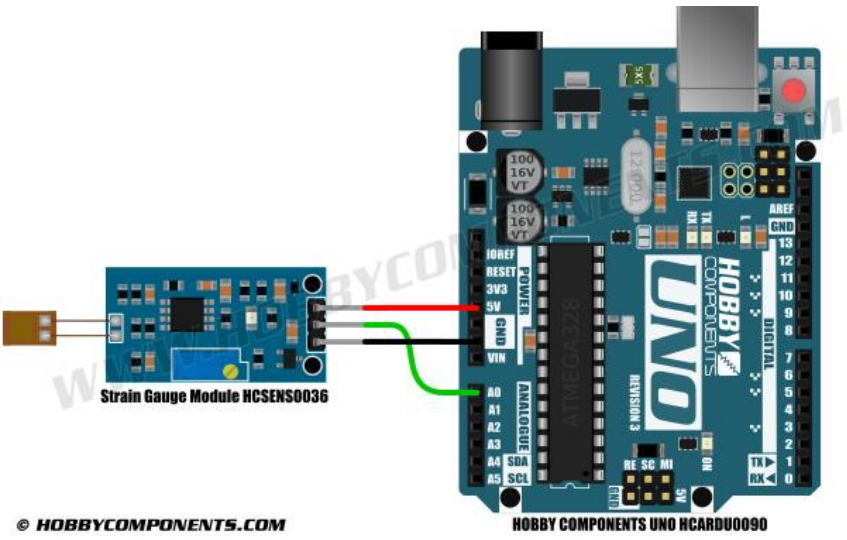

Figure 19.Assembly of the module with an Arduino UNO board (Source, Internet, [39])

4.1.3 Analog to digital converter ADC

When a microcontroller receives an analogue signal, automatically transforms it into a digital value, since it can't process it otherwise. The component in charge of this operation is the ADC.

Arduino UNO already contains 6 ADC on the board, with a resolution of 10 bits and, as has been mentioned previously, it works in a range of 0 to 5V. That means that the representation of 0V in binary values is 0000000000 (0 in decimal notation) and, on the other hand, 5V corresponds to the binary value of 1111111111 (1023 in decimal notation) [47]. If we divide 5V by 1023, the value $4{,}8875 \cdot 10^{-3}$ is obtained. This means that we can represent analogue values in decimal notation from 0 to 1023 with a resolution of 4,8875mV. Every time there is an increment or decrement of 4,8875mV, the microcontroller adds 1 in binary.

For some applications, this resolution could be good enough but the data that will be measured in this application, whether it's the electrical resistance or current, is expected to have increments that will not be perceived by the Arduino board by itself.

The chosen option to solve this problem has been a 24-bits ADC. Those converters use 24 bits for representing analogue values, meaning that they can represent 2^{24} (16.777.216) discrete levels and their resolution can be calculated with the following formula:

$$\frac{5V}{2^{24}} = 0{,}29802\mu V \ (1)$$

Besides the increment in the resolution, the use of an external ADC liberates the microprocessor from this duty. Thanks to that, the controller, which often has limited processing power, can focus on other tasks.

The 24-bit ADC acquired for this thesis has been an **ADS1256** from Texas Instruments [42], an ADC specifically designed for applications that require highly accurate and high-resolution analogue-to-digital conversion.

The ADC implements a low-noise programmable gain amplifier (PGA) that provides gains of 1, 2, 4, 8, 16, 32, or 64 in binary steps and a data rate from 2.5 to 30k samples per second (SPS), even though higher gains and data rates generate higher noise, with a maximum resolution of 23 bits noise-free with a gain of 1 and a data rate of 2.5 SPS.

Communication is done over an SPI serial interface thanks to the pins SCLK, DIN, DOUT, DRDY and CS. Those pins work all together to establish bidirectional communication. In a summarized way, the purposes of the pins are:

1. **SCLK (Serial Clock):** The SCLK pin acts as the clock signal for the serial exchange of data between the ADC and the Arduino board. During the communication of the devices, the master device (Arduino) generates clock pulses on the SCLK, to indicate when the ADS1256 should read or transmit data bits in a serial way, one by one, on each clock pulse.
2. **DIN (Data Input):** The Arduino board sends data to the ADS1256 through this pin and the ADC.
3. **DOUT (Data Output):** The ADS1256 transmits data to the Arduino board through this pin.
4. **DRDY (Data Ready):** The DRDY pin indicates to the Arduino board that new data is available to read. When the ADS1256 completes an analogic-to-digital conversion and the data is ready to read, the DRDY sets a “low” logic level to indicate that the conversion result is available. This behaviour can be observed in Figure 20, extracted from the ADS1256 datasheet [42], where the command RData (Read Data) is executed.

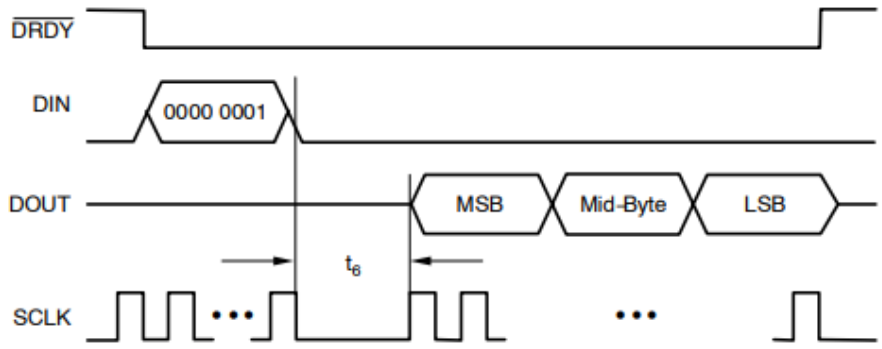

Figure 20. RDATA Command Sequence (Source: ADS1256 Datasheet [42])

After the DRDY pin goes low, the ADS1256 start reading the data and after a delay, t_6, said recorded data starts to shift out on the DOUT pin. When this process finishes, DRDY goes high again.

5. **CS (Chip Select):** This pin is used to initiate and control the communication between the Arduino board and the ADS1256. By selecting or deselecting the CS pin, the microcontroller can initiate and manage data transfer and commands between itself and the ADS1256 while interacting with other peripherals on the same SPI bus.

Additionally, the **PDWN (Power Down)** pin of the ADS1256 is used to control the power state, allowing to put the ADC into a low-power mode (consuming minimal power, reducing its functionality and stopping conversions. It is useful to conserve power or temporarily pause the ADC's operation.) or wake it up back to its full functionality.

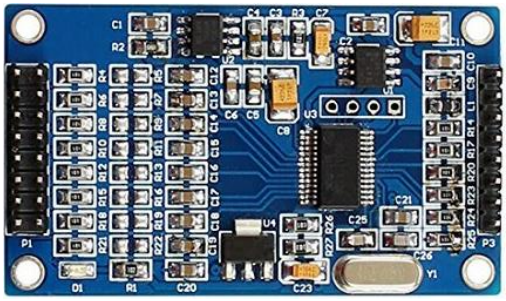

Figure 21. Very Low Noise, 24-Bit Analog-to-Digital Converter ADS1256 (Source: Internet [43])

The price of the ADS1256 is around **20€,** being a low-cost, high-performance solution for the thesis.

4.2 Electrical current sensor

With this solution, the electrical resistance will be calculated thanks to recording electrical current data and applying Ohm's Law.

When it comes to electrical current sensors compatible with Arduino, the main choices are **ACS758**, **INA219** and **ACS712**. In this chapter, a discussion will be performed to determine the more accurate sensor for the project that is about to be developed.

- **ACS758** [44]

This sensor consists of an integrated circuit designed for current measurement with frequencies that can reach up to 120kHz. The sensor generates an output voltage proportional to the current passing through it.

The ACS758 family offers sensors that can record currents up to 50, 100, 150 or 200A depending on the chosen device. This sensor can measure bidirectional current flow, which means that AC can be captured with it. This option would've been interesting if an AC supply could be obtained. For this thesis, it wasn't possible but for future works, it could be taken into consideration (See section *5.8 Using of AC vs DC*)

The price of this device is around **10€**

Despite all the prestation that it offers, this sensor is designed for measuring electrical currents way higher than expected for this project. This difference in magnitude could cause less accurate readings.

- **INA219** [45]

The INA219 current sensor can detect voltage, current and shunt power at the same time and send the data via I^2C protocol. It has a 12-bit Analog-to-Digital Converter (ADC) that converts the current recorded by a precision amplifier. It can measure currents up to ±3.2A, meaning that it can perform AC lectures, with a resolution of 0.8 mA.

Besides its versatility, it is mainly used for measuring the consumption of any Arduino project. When it comes to electrical current measurement, it needs an additional configuration besides the factory settings. Due to that reason, it is difficult to find existing applications of this sensor as a current one.

Its price, just like the sensor above, is around **10€**

- **ACS712** [46]

This sensor detects the magnetic field generated by the induction of an electrical current that is circulating on the component that is being measured, generating an output voltage proportional to it. It's able to record data from both AC and DC. Due to its easy assembly (it only has 3 pins, 2 for the power supply and the other one for the analogical output) and its price, around **8€**, it is the most used and documented sensor for measuring electrical current with an Arduino.

The ACS712 family consists of 3 different models, the ACS712-05A, the ACS712-20A and the ACS712-30A, for ranges of 5, 20 and 30A respectively. This is a significant difference compared with the ACS758, where the ranges were oversized for the application that the sensors will have on this project.

Due to its price, its large well-documented trajectory, and its adequate range of measurement, it's been decided to acquire the **ACS712** sensor for a range of **20A,** since the price difference between 5A and 20A was not significant and the 20A sensor provided more resolution compared to the 5A one (0.1V/A vs 0.185V/A) [47]

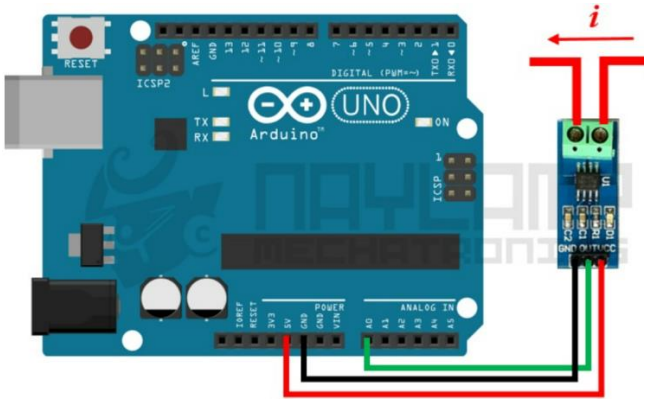

Figure 22.Mounting diagram of the electrical current sensor ACS712 on an Arduino UNO board (Source: Internet, [47])

All the sensors above are intrusive. That means that to measure the current, they must be placed on the electrical conductor. For the project that is about to be developed, this is not a deal breaker, since the specimen that is going to be used for measuring its electrical conductivity has two electrodes inside of it.

If we needed to measure the current in a non-invasive way, there are other options also compatible with Arduino such as the **STC-013** current sensor. This sensor allows the user to measure the current without having to disassemble the electrical conductor that is about to be measured. Its price is around **7€**. As has been mentioned, for this project it's not necessary to measure the current in a non-invasive way. Due to this, it has been decided

not to change the ACS712 for this sensor, since it will only increase the final price of the DAQ system.

4.2.1 Development of the electrical current sensor solution and why it couldn't be implemented.

As has been mentioned in section *4.2 Electrical current sensor solution*, the first option considered for this thesis was to record current data and after that, with Ohm's Law, transform said data into electrical resistance since the voltage supplied is known (5V, supplied by the Arduino board).

This option was considered in the first place since due that the applied voltage would be a constant value, the electrical current would be stable, and it will be easy to notice its changes.

For the electrical current solution, the device was wired as can be observed in the *Drawings* document, *Chapter 1. Current sensor solution*.

The sensor provided a voltage value through the ACD. Since the ACS712 reads a value of 2.5 volts for a current of 0A and it increases proportionally according to the sensitivity with a linear relationship between the voltage output and the current, the voltage values obtained can be translated into current values through the following formula [47]:

$$I = \frac{V_{OUT} - 2.5}{Sensibility} \quad (2)$$

Where the sensibility provided by the fabricator for the 20A ACS712 is 0.1V/A

The developed code can be found in the *Annexes* document, chapter *1. Annex I. Code,* section *1.1. Current sensor code* and its performance was checked with a lightbulb, a 5V battery and a multimeter. The DAQ system was able to measure the electrical current of the lightbulb but, when it came to the cement specimens, the data acquisition system couldn't detect the current of them since their electrical resistance was considerably high (around 3 to 4kΩ) and, therefore, the current between the electrodes was lower than the DAQ system could detect.

After this situation, it was decided to measure the electrical resistance with a voltage divider.

4.3 Voltage divider solution

After testing the electrical current solution and realizing that the data wasn't being recorded, another solution needed to be considered: a voltage divider.

Despite that a voltage divider is not as accurate as a current sensor for measuring absolute resistance values, it could still be considered an option since the object of interest was to record changes in the resistance value, not the value by itself.

Figure 23 illustrates the principle behind this solution.

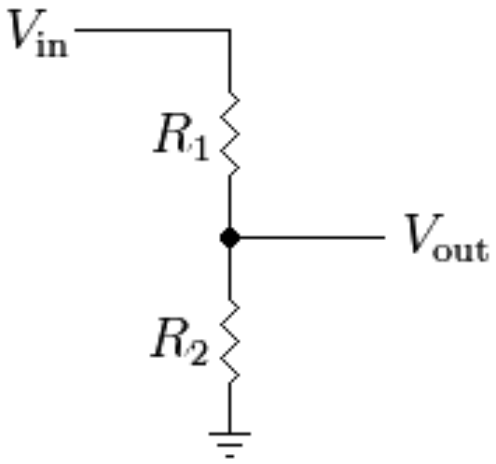

Figure 23. Voltage divider schematics (Source: Internet [48])

In the DAQ system that is about to be developed, the voltage provided by the Arduino board (5V) acts as V_{in}, a 5600 Ω resistor as the known resistor R_1, the voltage output registered by the Arduino board through the ADC as V_{out} and the cement specimens act as the unknown resistance R_2.

If Ohm's Law is applied and developed:

$$V = I \cdot R \quad (3)$$

$$I = \frac{V}{R} \quad (4)$$

Substituting (4) into (3) and in the case described in Figure 23:

$$V_{out} = V_{in} \frac{R_1}{(R_1+R_2)} \quad (5)$$

With some algebra, equation (5) can be transformed into equation (6).

$$R_2 = \left(\frac{V_{in}}{V_{out}} - 1\right) \cdot R_1 \quad (6)$$

In that way, thanks to a known resistor connected in series with the cement specimens, the electrical resistance of said specimen can be calculated thanks to the voltage output recorded through the 24-bit ADC.

5 Development and testing of the DAQ system

In this chapter, the development of the final design will be documented, from the wiring and programming of the microcontroller to the tests performed and their results. Even though this chapter has been divided into sections, these divisions are just to clarify the process of development of the data acquisition system and some of the following sections described have taken place simultaneously.

It can be considered that sections *5.1 Wiring, 5.2 Code* and *5.3 Excel set up* took place simultaneously, since changes in the code while it was being developed could be translated into changes in the wiring and vice-versa and the learning process about coding with Arduino was hand-in-hand with learning how to create data files with the recorded data.

Additionally, the sections considered above took place in parallel to sections *5.4 Preparation of the cement specimens* and *5.5 Assembly of the strain gauges*, which were consecutive processes.

Finally, when all the sections 5.1 *Wiring* to 5.5 *Assembly of the strain gauges* were finished, section *5.6 Cyclic load tests* were performed, and the results were analyzed in *section 5.7 Analysis of the recorded data.* For defending the use of AC, section *5.8 Using AC vs DC* was performed, closing in this way the experimental part of this thesis.

5.1 Wiring

Thanks to the Fritzing software tool, a wiring diagram of the Arduino board and the sensors has been performed. This diagram can be found in the document *Drawings, Chapter 2. Voltage divider solution.*

The development on how to wire the DAQ device can be found in the *Tor of Reference* document, chapter *2. Technical conditions*, section *2.4 Wiring requirements*.

Even though the developed DAQ system for electromechanical testing performs a very specific application, the individual wiring and coding (for further development of this issue see section *5.2 Code*) of each component of the data acquisition system are large well documented on IT sharing platforms such as GitHub and Arduino forums. Those platforms had a remarkable influence on the development of the thesis, working as starting point at the time of wiring the ADS1256 [49][50][51], the resistors [52], and both HCSENS0036 strain gauge modules [39].

5.2 Code

The developed code of the DAQ system can be found in the *Annexes* document, chapter *Annex I. Code,* section *1.2. Voltage divider code* document. This section has the purpose of making some remarks on said code.

1. As has been mentioned with priority in this thesis, the code was developed thanks to the work of other authors [49] [50] [51] [52] [39]
2. The language used to program the Arduino board was C++.
3. The SPI.h library used to develop the code is already installed on the development environment Arduino IDE. Nevertheless, the ADS1256.h library was developed by the GitHub user Axel Sepúlveda and can be found in his repository [50], which also contains examples of several codes for different applications of the ADC. His file,

ADS1256_Continuos_Reading_One_Channel, has been used as a starting point to develop the code of this thesis.

4. To use the library ADS1256.h, a C++ compiler needs to be installed on the computer. The compiler used in this thesis was Code::Blocks.
5. Both clockMHZ and vRef constant values can be found in the datasheet of the ADC.
6. The object adc contains the attributes *float clockspdMhz*, *float vref, bool useResetPin*
7. The function .begin() needs the three parameters *unsigned char drate*, *unsigned char gain* and *bool buffenable* (this last one refers to the ability of the ADC to temporarily store data from analogue to digital conversions before the microcontroller retrieves them or before transmitting them to another device).
8. The MUX register is the register in charge of controlling the input channel selection for the analogue-to-digital converter.
9. Since the HCSENS0036 strain gauge modules cannot be used to determine absolute measurements and can only provide relative changes, the outputs of the modules don't have units and can only take values from 0 to 1023 (the resolution of the Arduino board). For that reason, the code of the supplier [39] was complemented with a constant (5.0 / 1023.0), since the reference voltage of Arduino is 5V and the analogue lectures range is 1023 values. In this way, the unitless digital data provided by the modules is converted into a value between 0 to 5V.
10. The value of the unknown resistor (in this thesis, the cement specimen) has been calculated by applying Ohm's Law on a voltage divider as has been explained in section *4.3 Voltage divider solution*.

5.3 Excel set up

To facilitate the analysis of the extracted data from the DAQ system developed with Arduino, it has been decided to transfer said data to an Excel document. Thanks to the latest features of Excel, importing data from a device can be performed without any further complication. In this section how to connect and record data from an external device with Excel 2019 will be explained. (Note: This feature may not be available with older versions of Excel)

1. In a new Excel sheet, go to *File* → *Options.*

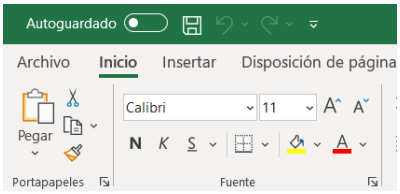

Figure 24. Excel screenshot 1 (Source: Own)

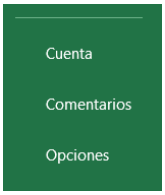

Figure 25. Excel screenshot 2 (Source: Own)

2. In the *Add-Ins* section, select *Manage → COM Add-Ins → Go.*

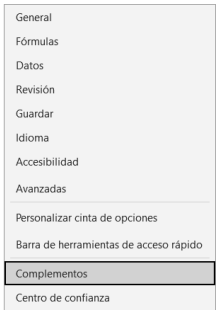

Figure 26. Excel screenshot 3 (Source: Own)

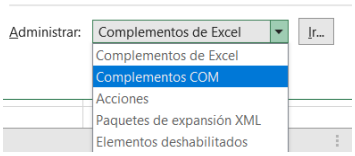

Figure 27. Excel screenshot 4 (Source: Own)

3. Select the *Microsoft Data Streamer for Excel* option.

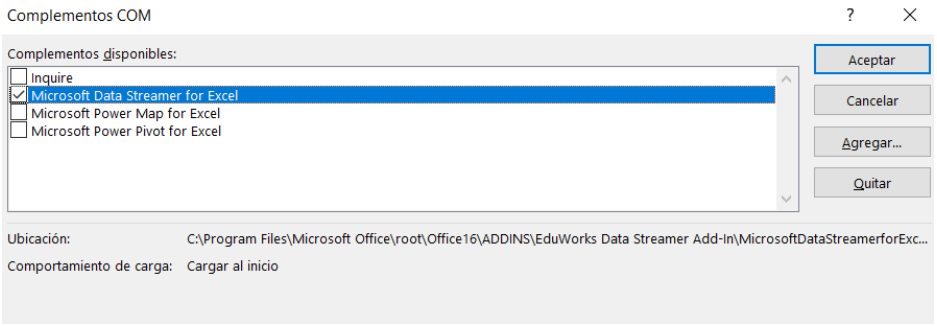

Figure 28. Excel screenshot 5 (Source: Own)

4. Acess to the new section on the toolbar, *Data Streamer*, and click on *Connect a Device*

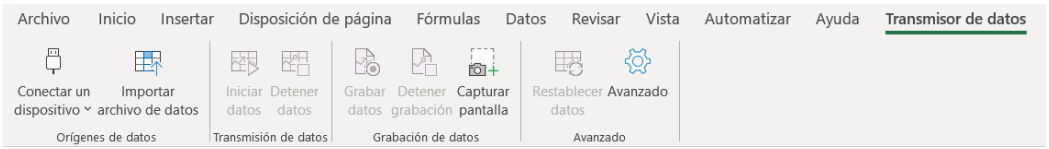

Figure 29. Excel screenshot 6 (Source: Own)

5. Select the Arduino board.

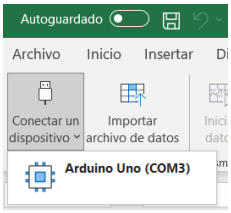

Figure 30. Excel screenshot 7 (Source: Own)

6. On the *Configuration* sheet, select the data frequency (between 10 and 1000ms between each lecture, the number of lectures that will be conserved (between 1 and 1000000), the number of channels for data entrance (a maximum of 1000 channels) and the orientation of the collected data (newest to last or last to newest). Figure 31 shows the configuration selected to perform the measurements in this thesis.

Figure 31. Excel screenshot 9 (Source: Own)

7. Click on *Start Data*

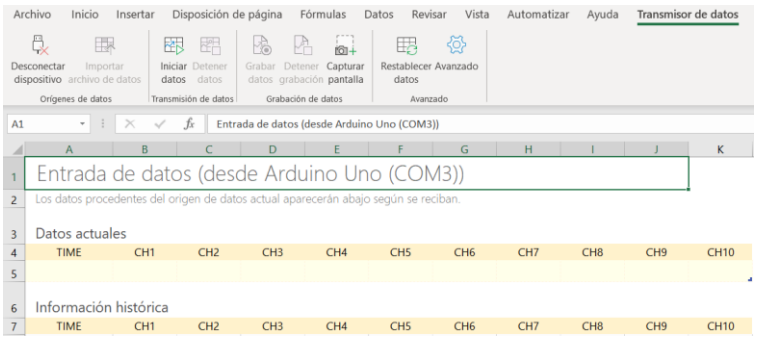

Figure 32. Excel screenshot 10 (Source: Own)

8. Click on *Record Data* and, after performing the necessary tests, click on *Stop Recording*

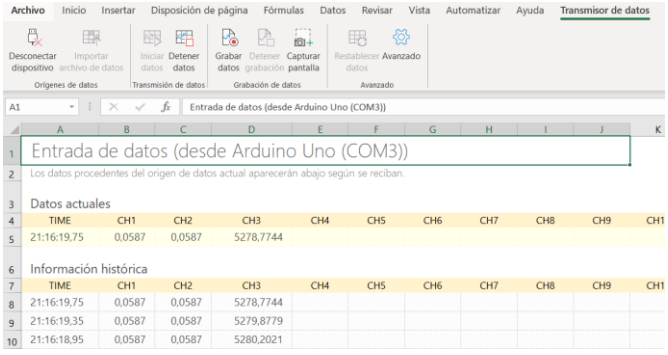

Figure 33. Excel screenshot 11 (Source: Own)

9. Excel will create a .csv file, a text file with the recorded data separated by commas.

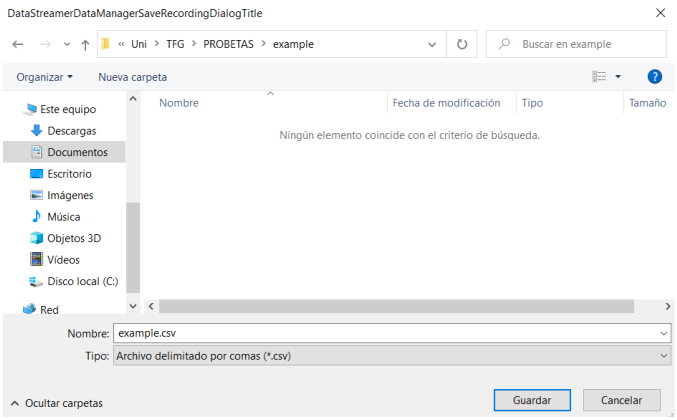

Figure 34. Excel screenshot 12 (Source: Own)

This file can be edited by any text editor, but it also can be opened on Excel following the next steps:

10. Open the .csv file with Excel and select *Next* on the emerging window.

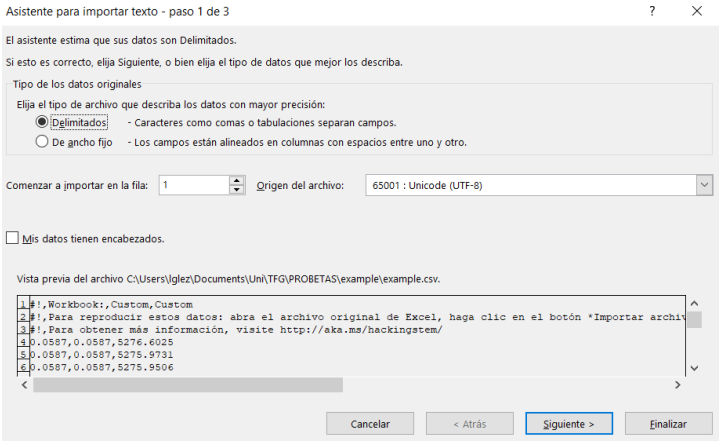

Figure 35. Excel screenshot 13 (Source: Own)

11. Set "*coma*" as the separator and click *Next.*

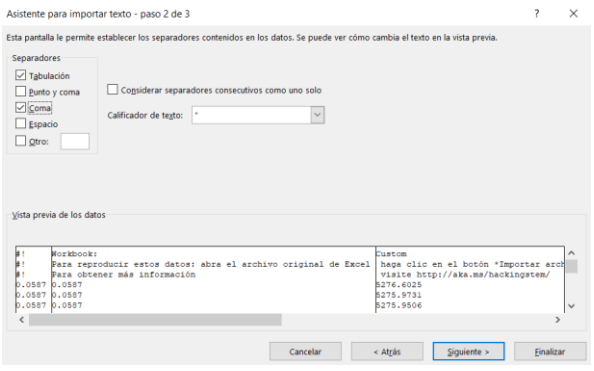

Figure 36. Excel screenshot 14 (Source: Own)

12. Click on *Advanced* and select a dot as a decimal separator and a blank space as a thousand separator.

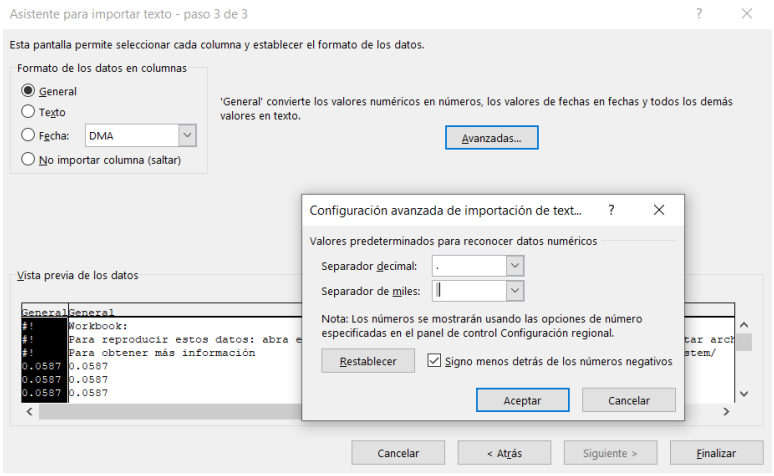

Figure 37. Excel screenshot 15 (Source: Own)

As can be seen in Figure 38, the .csv file is now separated into columns and the data is ready to be processed.

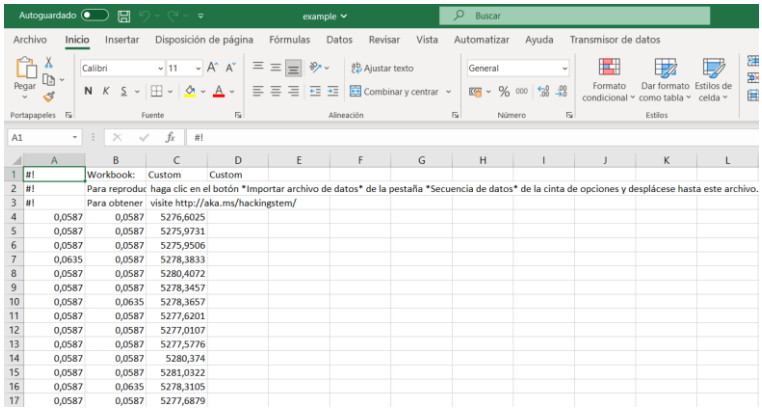

Figure 38. Excel screenshot 16 (Source: Own)

Note that, although Figure 31 shows the configuration used to record data on the cyclic load tests, the rest of the screenshots are just an example used to explain how to configure Excel for the application of this thesis. In no case, the data showed in these screenshots has to be considered as data recorded during the experimental part of this thesis.

5.4 Preparation of the cement specimens

Since the scope of this thesis is to design and implement a DAQ system for electromechanical testing, the preparation of the cement specimens was performed by the lab technician from the Department of Resistance of Materials and Structures. The preparation was documented, and it will be explained in his section.

For the preparation of the specimens, 3 kg of cement without aggregates was mixed with 1.3L of water. Since aggregates don't conduct electricity, by eliminating them, the conductive surface increases.

Figure 39. Cement weighing (Source: Own)

Figure 40. Cement and water mixing (Source: Own)

The mix was transposed into two wooden molds (previously covered by a mineral oil to facilitate the demolding of the specimens), with 3 holes of 5x5x5cm^3 each one marked with a line 2cm from each end, to place the electrodes in the center of the specimens. The molds were half filled with the cement, then, with a bolt, they were compacted and finally, they were filled with the rest of the mix and compacted again to uniform the specimens.

Figure 41. Molds with marks for the electrodes (Source: Own)

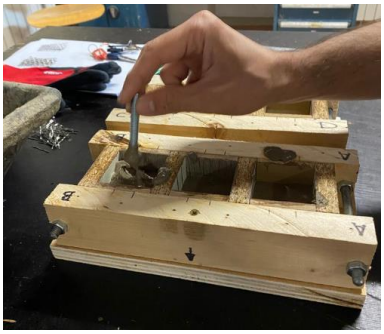

Figure 42.Compaction of the cement (Source: Own)

After removing the excess cement, the electrodes, (conformed by a mesh of stainless steel made of wires one millimeter thick separated 5 mm from each one, conforming in this way apertures of 5x5mm^2. Figure 43 illustrates this configuration.) were left to dry for 3 days under a plastic cover to avoid the evaporation of water, which could cause fissures.

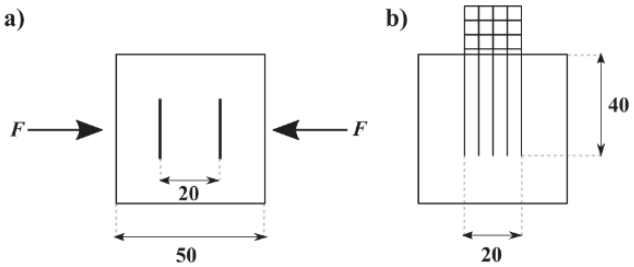

Figure 43. Schematic of electromechanical measurement setup for cubic specimens: a) arrangement of embedded mesh electrodes with respect to loading force F. b) Cross section of specimen showing embedded mesh electrode. Dimensions in mm. (Source: Design of a smart lime mortar with conductive micro and nano fillers for structural health monitoring [12])

Figure 44. Electrodes placed on the specimens (Source: Own)

Figure 45. Specimens left to dry with a plastic cover (Source: Own)

Since cement is a porous material, the excess water of the mix fills said pores, being responsible for the conduction of electricity of the material. As the mixture dries and loses water, the electrical resistance increases.

5.5 Assembly of the strain gauges

Once the specimens were dry and demolded, they were marked with a number from 1 to 6 to identify them and the strain gauges were installed thanks to the help of the lab technician from the Department of Resistance of Materials and Structures. The material requirements were:

- Isopropyl alcohol
- Loctite super glue
- Adhesive tape
- Strain gauges
- Multimeter
- Teflon sheet
- Cement specimens

In Figure 46, the materials listed above can be observed.

Figure 46. Strain gauges installation set up (Source: Own)

As can be observed in Figure 46, just 10 strain gauges arrived and, since the specimens needed 2 gauges each, the strain gauges could just be installed in **5 out of 6** specimens.

Firstly, the specimens were cleaned with the isopropyl alcohol, and marked with a pencil so the gauges will be centred between the two electrodes.

Figure 47. Cleaning of the specimens (Source: Own)

Afterwards, the gauge was taped into the adhesive tape. In that way, the possibility of touching the superglue with the hands was reduced. A drop of Loctite was placed where the strain gauge was going to be installed and, with the help of the tape, the stain gauge was placed on top of it, along the loading direction of the posteriors cyclic load tests. Next, with the Teflon sheet, the possible bubbles that could reside between the specimen and the gauge were eliminated.

Figure 48. Installation of a gauge (Source: Own)

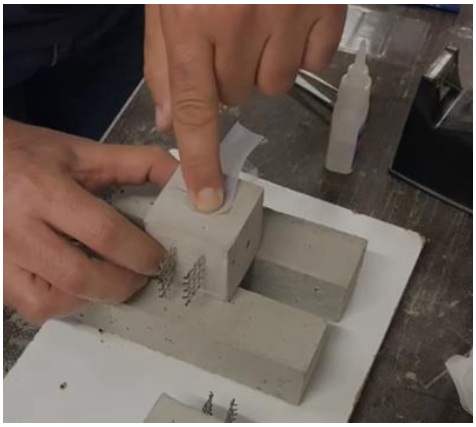

Figure 49. Elimination of bubbles (Source: Own)

Finally, to check that the strain gauges haven't suffered any damage during the installation, their electrical resistance was checked with a multimeter and compared with the electrical resistance provided by the supplier when the gauge wasn't experimenting any load.

Figure 50. Gauges datasheet (Source: Fabricator)

Figure 51. Electrical resistance lecture of the installed gauge (Source: Own)

As can be observed in both Figures 50 and 51, the resistance of the gauge is 350Ω, the same that the fabricator provided. In this way, the installation of the gauge can be considered successful.

The procediment described above was repeated for the 10 gauges available.

On a different day, and still thanks to the help of the lab technician from the Department of Resistance of Materials and Structures, two cables were welded to each strain gauge.

This part of the procedure implied more complications than the installation of the gauges on the specimens by itself. Since the welding process implied the use of heat to melt the tin, the glue used to install the gauges was dissolved as the welding process took place. This made some of the gauges detach from the specimens. Also, the weld of each gauge couldn't be in touch with each other and, since the space between the ends of the gauge is considerably limited, this implied that some welding process had to be repeated several times, implying an overheating of the gauges that led to the breakage of some of them.

At the end of this procedure and, with the complications mentioned above, out of the 5 specimens that had gauges installed, just one could be wired in both gauges, and the other two could be wired in just one gauge.

Table 5 summarizes the state of the specimens at this point of the thesis and Figure 52 shows a close-up of the specimen with both strain gauges wired, from now on Specimen 3.

Initial specimens	Specimens with strain gauges	Specimens with wires	
		2 gauges wired	1 gauge wired

Table 4. State of the cement specimens (Source: Own)

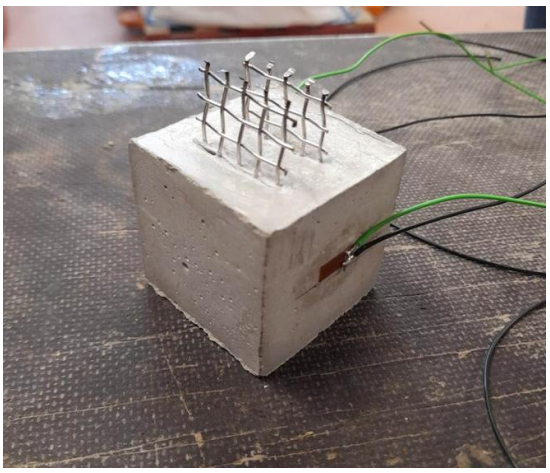

Figure 52. Close-up of Specimen 3 (Source: Own)

5.6 Cyclic load tests

With the DAQ system already developed and the specimens ready to be used, cyclic load tests could be performed on **3 out of the 6 initial specimens**. The tests were performed on **Specimen 3** and two specimens with just 1 gauge wired, and from now on **Specimen 1** and **Specimen 4**.

The bench vice has a force limit, ensuring that the same peak force was applied to all specimens.

Two wooden pieces were placed between the specimens and the vice, to avoid the interaction between the electrical voltage that was being applied to the specimens and the metal surfaces of the vice that could alter the lectures. This setup can be observed in Figure 53.

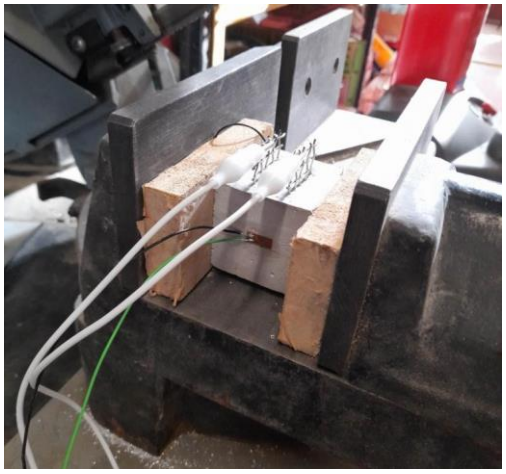

Figure 53. Placement of two wooden pieces between the vice and the specimens (Source: Own)

The gauges were connected to the two strain gauge modules and, thanks to the two crocodile cables connected to the electrodes, the voltage divider configuration was completed (Figure 54). For a cleaner explanation of the wiring see section *5.1 Wiring diagram*.

Figure 54. DAQ system set up (Source: Own)

The tests were performed on the three specimens mentioned before and strain and resistance data were collected. Now, in section *5.7 Analysis of the recorded data,* the experimental results are going to be exposed.

5.7 Analysis of the recorded data

The procedure followed to process the data can be listed as:

1. Calculate the increment of voltage output for the first strain gauge (subtracting the value of the first lecture from every other value).
2. Calculate the increment of voltage output for the second strain gauge. This step was just implemented in Specimen 3 since is the only one with two strain gauges installed.
3. Calculate the average between the increments of both gauges and divide the obtained value by 1000, the value of gain of the strain gauge module [53], to obtain the actual value of the voltage output. When there is just one gauge, instead of on an average, this division will be performed just on the increment values of said gauge.
4. The lectures of the gauges can be transformed into deformation measurements thanks to the quarter bridge formula [54]:

$$\varepsilon = -\frac{4 \cdot \Delta V}{V_{REF} \cdot \lambda} \quad (7)$$

   Where ΔV has been calculated with priority, V_{REF} is the voltage of reference from the Arduino board, 5V, and the gauge factor λ is provided by the gauge fabricator (See Figure 50).

   Note that the formula described above contains a negative symbol. This is due that, while resistance and strain data should be synchronous, one particularity of the strain gauge modules used is that when they detect a compression effort, its output voltage value increases. By adding a negative symbol to the deformation formula, this particularity can be sorted out and the deformation values can be calculated.

5. Calculate the increment of resistance for the specimen and divide said value by the value of the first lecture to obtain the fractional increment of resistance of each lecture.

With the transformations explained above, three kinds of graphs were performed for each specimen:

1. **V1, V2 and R time history**. Represents the evolution of voltage of the first and second strain gauge and resistance data as it was being recorded.
2. **ΔR/R and ε time history**. To show the evolution and the relation between resistance and deformation.
3. **ΔR/R vs ε**. The gauge factor is the relation between the fractional change in the resistance values and the deformation [55]. By correlating both data and determining the slope of the obtained trend line, the gauge factor of each specimen can be calculated.

While in this report document, only the graphs of the last tests will be displayed, the graphs of all the essays can be found in the *Annexes* document, chapter *2. Annex II. Graphs.*

5.7.1 Specimen 1

Three tests were performed on Specimen 1 while recording electrical resistance and strain data from its only strain gauge. The evolution of the graphs show that the resistance value increased with time until they got stable on the third test. As can be observed, the application of a load was translated into a change in resistance. When a compression effort was being applied the value of resistance decreased, since the electrodes of the specimen were closer to each other, while the output values of the strain gauges modules increased, due to the peculiarity explained in section *5.7 Analysis of the recorded data.*

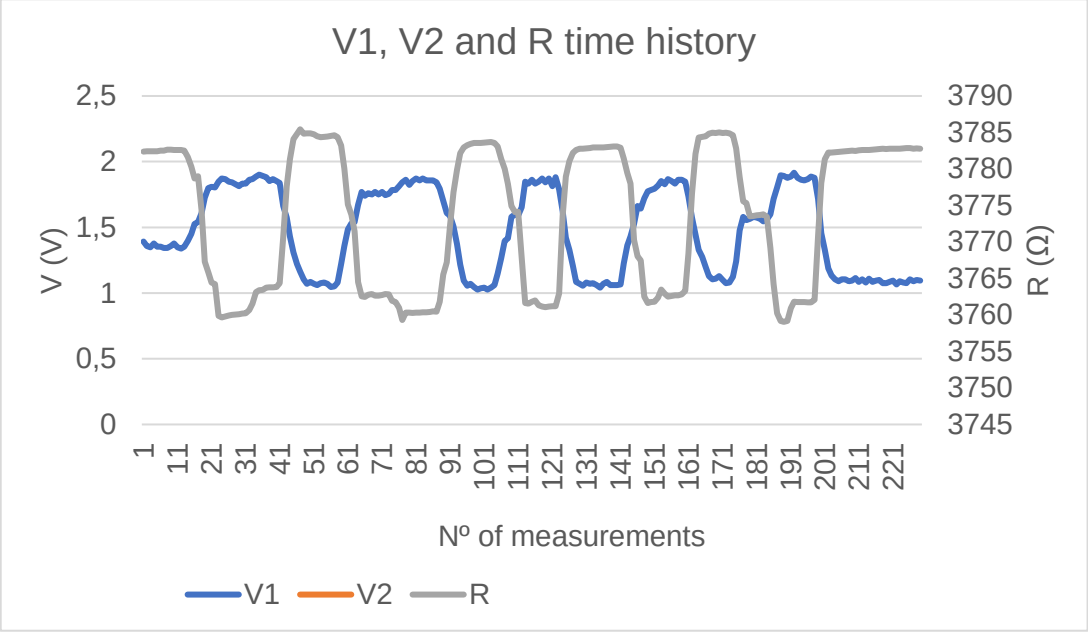

Figure 55. V1 vs V2 vs R graph for the third test on Specimen 1 (Source: Own)

After performing the transformations mentioned in section *5.7 Analysis of the recorded data*, the relationship between deformation and fractional change on the resistance can be observed in a more clarifying way. The *ΔR/R0 and ε time history* graph in *Figure 56* shows how the application of a load, and therefore the deformation of the specimen, was translated into a change in the fractional value of the resistance regarding its original value.

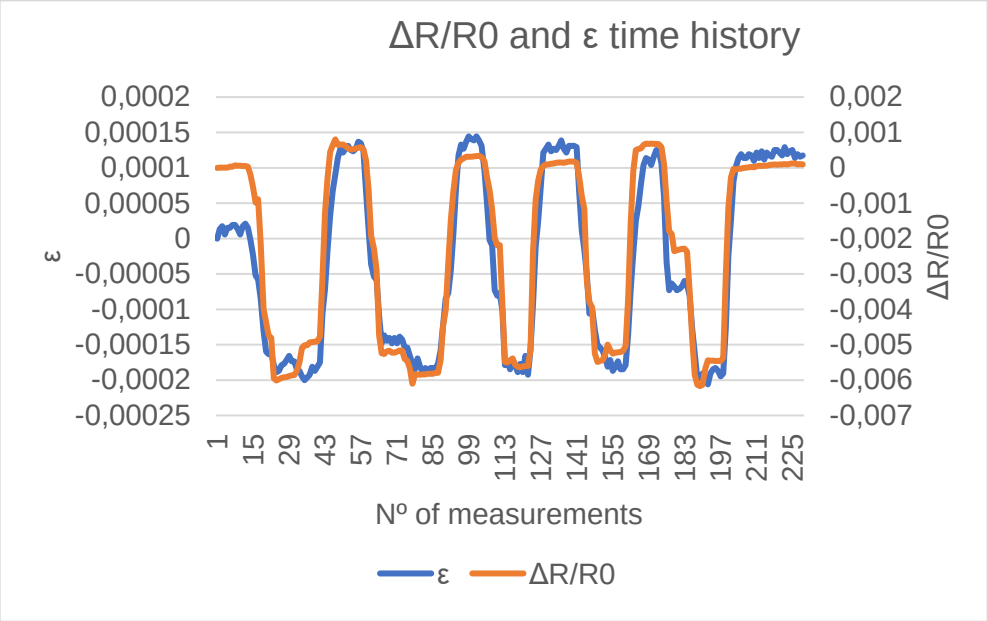

Figure 56. ΔR/R0 vs ε graph for the third test on Specimen 1 (Source: Own)

With the dispersion graph, the correlation between both data can be observed. As the cyclical tests were performed, it can be observed that the transitory state was left behind, and the recorded data stated to acquire stability and the values of ΔR/R0 and ε started to be placed closer to the trendline, with notorious emphasis on the extremes of it. The R^2 coefficient for this test was above 0,9. In this way, a linear relationship between the deformation and fractional change of the electrical resistance can be assumed.

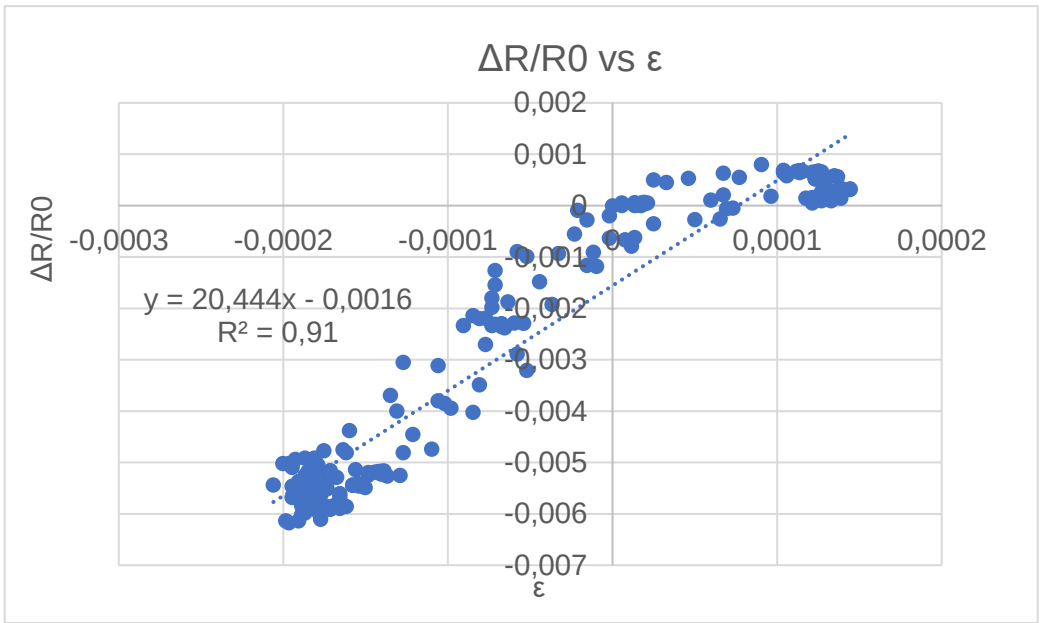

Figure 57. Dispersion graph ΔR/R0 vs ε for the third test on Specimen 1 (Source: Own)

After looking at the slope of the trendline of Specimen 1, its gauge factor can be determined as:

$$\lambda_1 = 20{,}444 \quad (8)$$

5.7.2 Specimen 3

As has been mentioned in section *5.5 Assembly of the strain gauges,* Specimen 3 is the only cement specimen with two strain gauges attached.

Four consecutive cyclic load tests were conducted in this specimen. It can be observed that, just as in Specimen 1, as the tests took place, the value of the resistance increased and got stabilized.

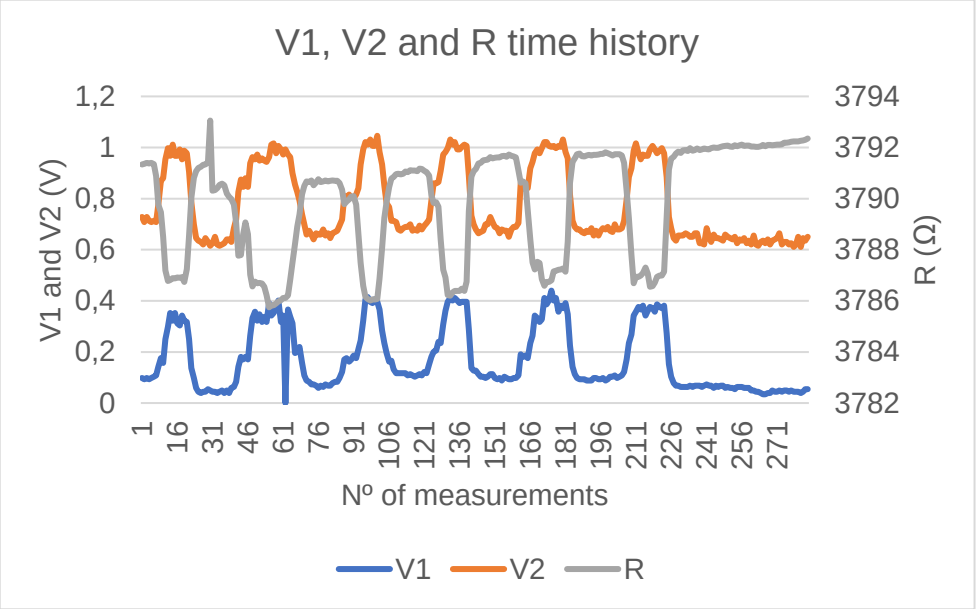

Figure 58. V1 vs V2 vs R graph for the fourth test on Specimen 3 (Source: Own)

Equation (7) was applied to the recorded data the results exhibited the same behaviour as Specimen 1.

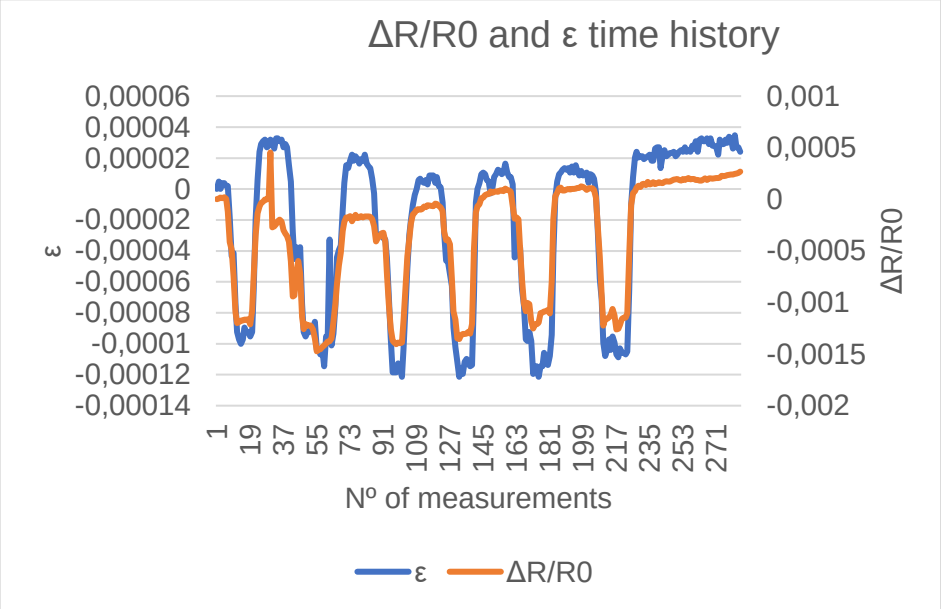

Figure 59. ΔR/R0 vs ε graph for the fourth test on Specimen 3 (Source: Own)

Finally, with the dispersion graph, an R^2 coefficient above 0,9 is obtained again. Therefore, the same made with Specimen 3 can be applied in this scenario: the deformation and the fractional change of the electrical resistance are linearly related.

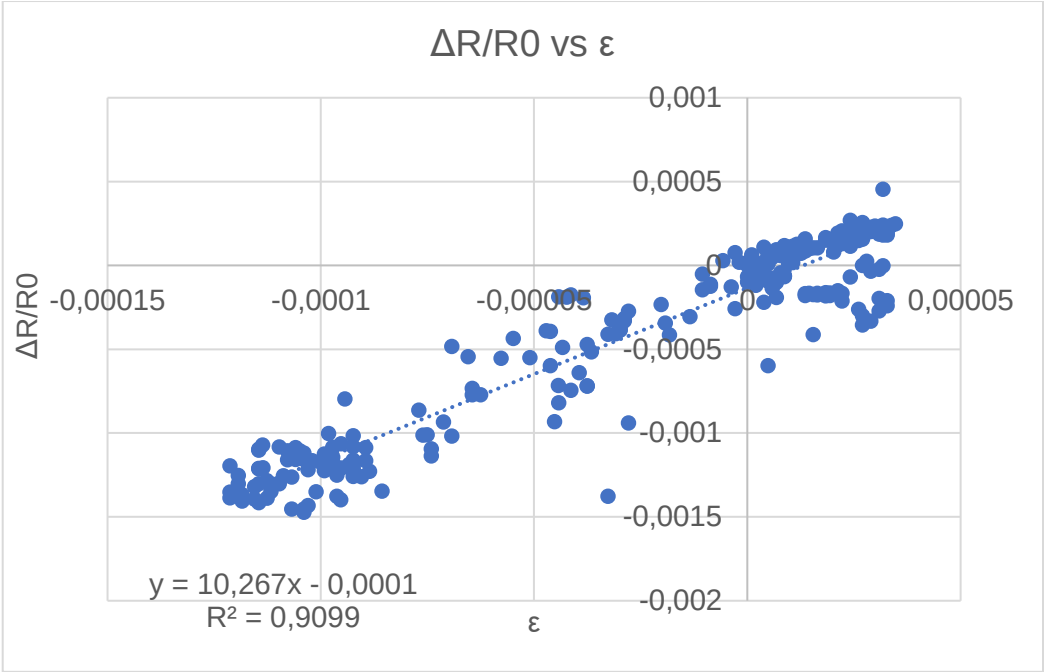

Figure 60. Dispersion graph ΔR/R0 vs ε for the fourth test on Specimen 3 (Source: Own)

The slope of the graph in Figure 60 sets the gauge factor for Specimen 3 as:

$$\lambda_3 = 10{,}267 \quad (9)$$

5.7.3 Specimen 4

When the first test was being performed on Specimen 4, its only gauge fell off. This was caused by the complications of the installation mentioned in section *5.5 Assembly of the strain gauges*. The gauge couldn't be re-installed, and the graphs in the *Annexes* document, chapter *2. Annex II. Graphs,* section *2.3. Specimen 4* show the irregularities caused by the disconnection.

Due to this, no conclusion could be extracted since the cyclic load tests couldn't be performed and Specimen 4 couldn't be characterized.

5.7.4 Obtained results summary and interpretation

This section aims to summarize the results extracted data from subsections *5.7.1 Specimen 1*, *5.7.2 Specimen 3* and *5.7.3 Specimen 4*

Firstly, an overview of the obtained gauge factors will be presented in Table 6.

Specimen	Gauge factor λ
1	20,444
3	10,267
4	Couldn't be determined
Mean	**15,356**

Table 5. Overview of the obtained gauge factors (Source: Own)

As has been explained in subsection *2.2.1 Strain and damage sensing*, the gauge factor is an indicator of the piezoresistive effect during mechanical loading. A higher gauge factor indicates higher sensitivity of the material's electrical resistivity to applied axial strain.

This can be observed on the ΔR/R0 and ε history time graphs for both specimens (Figure 56 and Figure 59), where the deformation changes were translated into higher changes in the fractional value of resistance for Specimen 1 than Specimen 3. In this way, it can be concluded that Specimen 1 is "smarter" than Specimen 3 since it has more sensibility at the time of translating deformation changes into electrical resistance changes.

Table 6 illustrates how the mean between the gauge factor of Specimens 1 and 3, 15,356, is approximately 7,5 times bigger than the gauge factor of the strain gauge, 2,03, meaning that both specimens were more sensible to detect damage than the strain gauges.

It can be concluded that the low-cost DAQ system was able to monitor the specimens and that deformations could be detected by the decreasing the resistance values.

Having characterised the gauge factor of these specimens using the DAQ system, these specimens can be used as smart sensors embedded in a concrete structure. The monitoring of the structure with these sensors can be subsequently performed using the same DAQ system.

5.8 Using AC vs DC

As has been said previously in this thesis, the development of this thesis was limited by the lack of availability of an AC power supply.

Cement is a dielectric insulator material. When a dielectric material is placed in an electric field, the electric charges don't flow through the material since they don't have free electrons. Instead, they are slightly shifted from their equilibrium positions, causing dielectric polarization. Due to that, positive charges move in the direction of the field and negative charges move in the opposite direction of the field. This polarization creates a strong internal field that reduces the overall electric field within the material. [56]

In their work *Elimination of polarization effect in DC measurement of resistivity of CNT-cement composites* [57], Tamov et al explain that, during the application of a DC on cement-based materials, the polarization-induced electric field generated in the material as a response to the applied electric field of the DC has an opposite direction regarding the applied electric field. This polarization results in the growth of measured resistivity with time during resistivity measurement.

This effect causes difficulties in associating the changes in resistivity with the application of a load since it makes it trickier to determine if the changes in resistivity are due to the appearance of deformation or caused by polarization.

The authors also mention that applying voltage signals with alternating current signals with equal magnitudes of positive and negative peaks can reduce or eliminate the polarization, even though it's a more complicated process since it's necessary to establish the appropriate current frequency to avoid the polarization effect and AC measurements are made with more sophisticated equipment as compared to DC measurements.

Note that even in the paper mentioned above the authors offered a solution for the polarization effect in DC measurements, it cannot be applied to this thesis, since the solution purposed is for static loads. (Set the frequency of the measurements up to 5 minutes).

The day after performing the tests, Specimen 6 was left for approximately a day to record its resistance values.

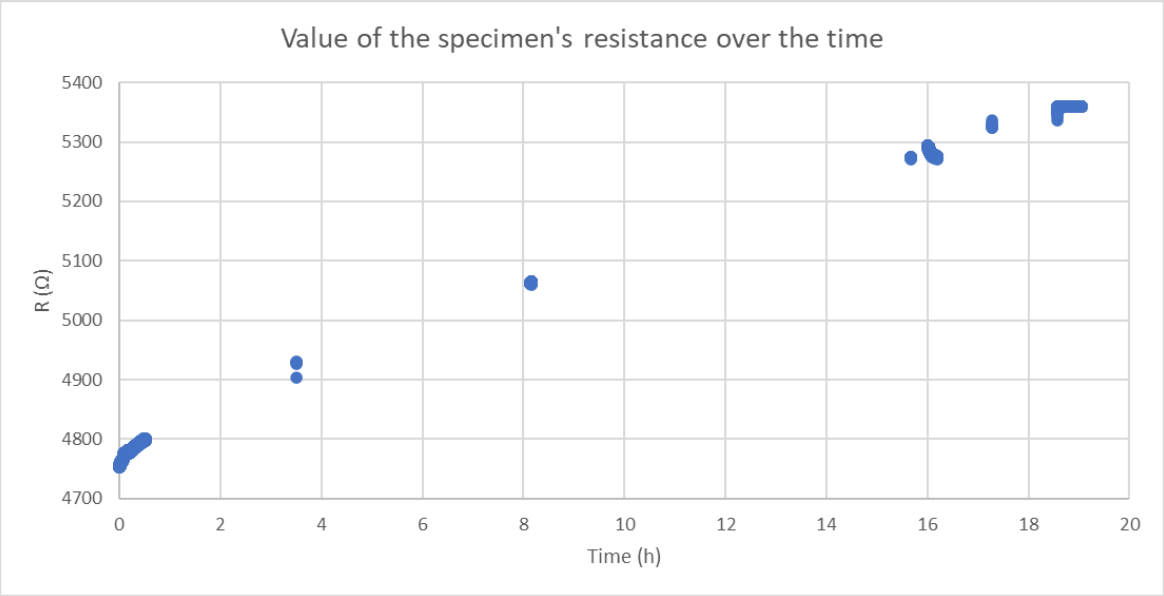

Figure 61. Specimen's 6 resistance over the time (Source: Own)

As can be observed in Figure 61, the value of the resistance increases as time goes by. Since the cement specimens had been demolded 3 days after their preparation and the tests were performed approximately one month after the demolding, it can be considered that the specimens still experiencing hydration and carbonation. The hydration process produces ions that remain trapped in the hardened parts of the cement. Additionally, the carbonation process (consisting of the reaction between the calcium hydroxide and the carbon dioxide of the atmosphere) generates calcium carbonate and water molecules, that, under the application of a DC, can be ionized as well. Overall, during this process, several ions such as OH^-, Ca^{2+} and Cl^- are created. These ions are affected by the DC, and due to that reason, the chin into the resistance is considerately pronounced. To avoid this phenomenon, it would be an interesting topic for future works to acquire an AC power supply and compare the obtained results with the DC ones.

6 Budget summary

This section aims to summarize the budget dedicated to this thesis.

The budget has been divided into two different cost categories. The first one includes the human resources costs, referring to the time invested into the development of the thesis and the fees of the people involved in it. The second one is about the costs of the materials (including hardware and software) involved in the development of the DAQ system.

Table 8 shows the costs of said sections and the total cost of the thesis. For further details, see the *Budget* document.

Section	Cost (€)
Human resources	5.622,50
Material costs	231,03
Total cost	**5.853,53**

Table 6. Budget summary (Source: Budget document)

7 Analysis and assessment of environmental and social implications

7.1 Carbon footprint of cement

This thesis is focused on the development of a low-cost data acquisition system for electromechanical testing of smart materials. In this chapter, a study about the carbon footprint of said materials will be performed.

Cement is obtained by breaking down limestone and other calcareous materials, a reaction that occurs at more than 1400ºC, generating clinker: a granular material and the main component of common cement. When this temperature is reached, the clinker releases the carbon trapped inside and, in contact with air, it turns into CO_2, which rises into the atmosphere and contributes to the greenhouse gas effect. [58]

Nowadays, the fabrication of cement represents 8% of global CO_2 emissions according to the International Energy Agency, being one of the sectors that contributes the most to these emissions. Its carbon footprint can be estimated as 0,913 tons of CO_{2eq} for each ton of cement where 0,47 tons of CO_2 come from the chemical reaction that produces the clinker and the rest come from the necessary energy to produce the reaction since, as has been said, the ovens in which it occurs must reach 1400°C and the use of fossil fuels is needed. [59]

Despite these emissions, production doesn't stop. Every year, 4.100 million tons of cement are generated. With this amount of generation, plus the carbon footprint mentioned above, the emissions of the cement industry can be compared to the emission of a country. If this industry were a country, it would be the third largest emitter in the world behind China and the US. [60]

In today's society, the use of concrete seems indispensable for the construction industry. The explanation to this can be found in the words of Felix Preston, deputy director of research at Chatham House's Department of Energy, Environment and Resources:

"It is affordable, can be produced almost anywhere, and has all the right structural qualities to construct a durable building or infrastructure [...] Building without it, while possible, is challenging" [61]

To mitigate these effects, in 2021, the Global Cement and Concrete Association (GCCA), which represents 35% of the world's cement production capacity, launched the 2050 Cement and Concrete Industry Roadmap for Net Zero Concrete. The GCCA compromised to cut CO_2 emissions by a further 25% by 2030 and reach 0 emissions by 2050.

The pathway that GCCA will follow can be summarized in Figure 62:

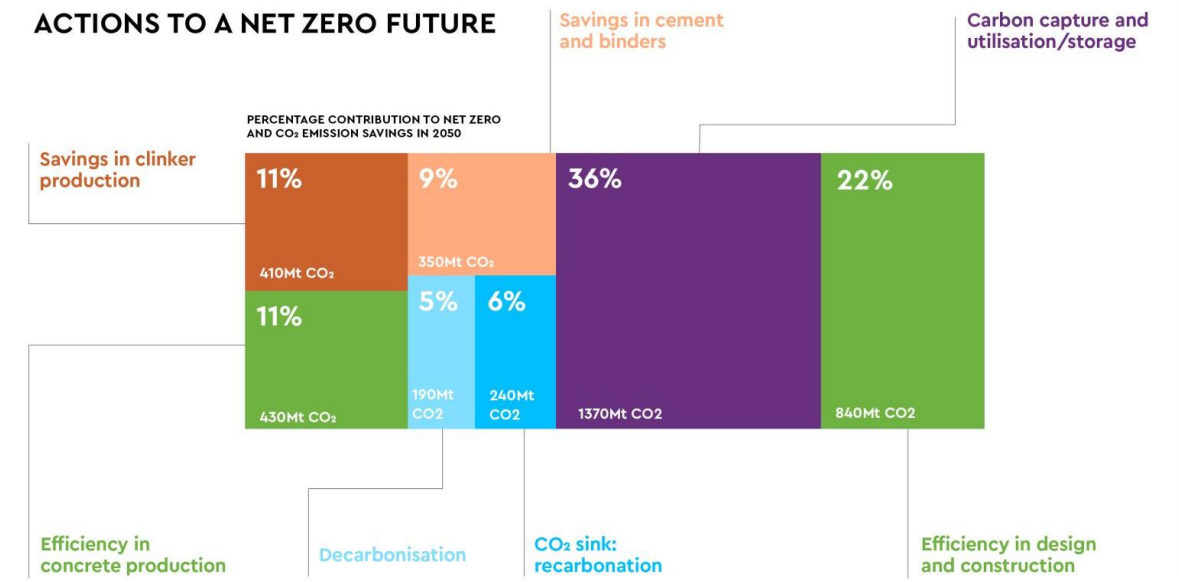

Figure 62. Actions to a Net Zero future (Source: Internet [62])

As can be observed, the road to a Net Zero future has 7 main areas of action: saving in clinker production, efficiency in concrete production, decarbonization, CO_2 sink: recarbonation, saving in cement and blinders, carbon capture and utilization/storage and efficiency in design and construction.

Taking into consideration the field that this thesis is involved in, the area that has more interest is the second one which will imply bigger savings on CO_2 and **efficiency in design and construction**. This area, according to GCCA, consists of 4 different sub-areas of actuation [62]:

- client brief to designers to enable optimization.
- design optimization.
- construction site efficiencies.
- re-use and lifetime extension.

Focusing now on lifetime extension, the next chapter of this thesis will illustrate how monitoring a structure can extend its lifetime through **preventive maintenance**.

7.2 Preventive maintenance

Preventive maintenance is a form of maintenance that implies periodicity. It is performed regularly and routinely on any kind of component that may require it and, thanks to it, the chances of equipment failure or unplanned downtime. Those failures can be very expensive to solve, and thanks to preventive maintenance, they can be avoided.

To illustrate how preventive maintenance can be helpful when it comes to extending the lifetime of a structure, it is of interest for this thesis to mention a paper from Li, J. et al.: *Automated decision-making in highway pavement preventive maintenance based on deep learning* [63]. Despite being about highway pavement, the conclusions reached in it apply to any kind of structure or structural component.

In their paper, among other research, the authors compared the behavior of pavement when preventive maintenance is applied versus when corrective maintenance (maintenance that

only occurs when, in this case, the pavement, has suffered serious damage) and the lifetime of the pavement with both methods.

Li, J. et al. elaborated a diagram that illustrates the benefits of preventive maintenance versus corrective maintenance:

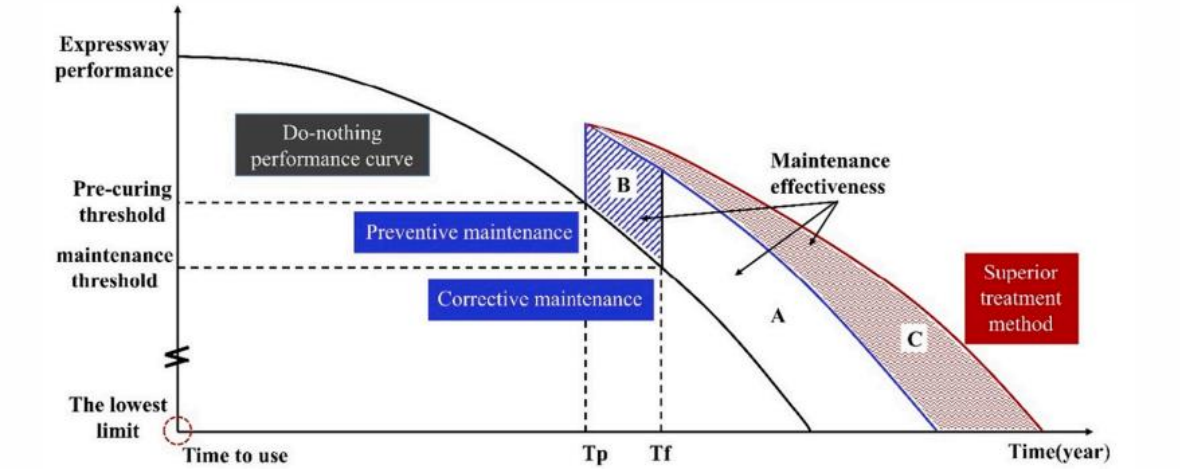

Figure 63. Influence of preventive maintenance and corrective maintenance on pavement performance (Source: Automated decision making in highway pavement preventive maintenance based on deep learning [63])

Where the elements that can be observed are the following:

- **Black curve**: Decay curve. The component, in this case, the pavement, will continue to deteriorate over time.
- **Area A**: Benefit of corrective maintenance.
- **Area B**: Additional benefit of preventive maintenance
- **Area C**: Benefit if appropriate maintenance methods are taken to reduce the deterioration ratio of the performance decay curve.

As can be observed, preventive maintenance of a component (in the case of this thesis, a structural component) can significantly extend its lifetime, implying economic and material savings.

Preventive maintenance can be performed in more than one way. It can be time-based, usage-based, or condition-based.

Time-based preventive maintenance, as its name indicates, consists of scheduling preventive maintenance tasks using a set time interval, such as every 10 days, the first day of every month or with any time frequency that the company deems necessary.

Usage-based preventive maintenance is performed when a certain benchmark of usage is reached. This could be a certain number of kilometres, production cycles or whatever parameter that needs to be controlled.

Finally, condition-based preventive maintenance is a maintenance strategy that monitors the condition of the component that would be subjected to preventive maintenance and determines what maintenance task needs to be done when certain indicators show signs of

decreasing performance or upcoming failure. This type of preventive maintenance is also known as **predictive maintenance** and is the one of most interest for this thesis. [64]

Predictive maintenance, as has been mentioned above, implies the use of a monitoring system that is used during regular operations. Thanks to this monitoring, the chances of a breakdown can be markedly reduced. The main goal of predictive maintenance is to predict equipment failures and take corrective measures, increasing the useful life of a product or component.

The main components of predictive maintenance are [65]:

Condition-Monitoring Sensors

The sensors are responsible for monitoring the component and providing real-time data and tracking maintenance needs from inside the equipment without disrupting operations.

The Internet of Things (IoT)

The data collected by the sensors can be shared through the Internet of Things. Predictive maintenance is composed of a network of sensors all working in tune with each other. To be able to analyze all the data from the different sensors that conform to the condition-monitoring system, it is necessary to store this information in a centralized storage system, whether in a local area network or using cloud technology.

Predictive Formulas

Predictive algorithms analyze the collected data and identify trends to compare the current behaviour with its expected one and report when the component that is being monitored will need to be repaired or replaced. Thanks to this detection on early-stage, technicians can intervene and prevent massive breakdowns.

But what makes predictive maintenance stand out above the other kinds of preventive maintenance?

With preventive maintenance, the data that is available for the technicians is just general information available for the model of the component that will be submitted to maintenance. With this, just approximately predictions of when to realize the maintenance can be performed.

On the other hand, predictive maintenance is considerably more accurate and due to this, it requires more data. Information about the expected lifecycle of the component that is submitted to maintenance is combined with historical data about the performance of that unit and, thanks to the IoT technology mentioned above, constant updates about the activities of the monitoring system are generated. This additional information allows generating of predictive models with strong accuracy that allow the technicians to know with certainty when system failures will occur. [66]

Because with predictive maintenance repairs are being scheduled exactly when needed and not according to a general timetable, this implies that no unnecessary repairs are made. In this way a significant amount of time, waste in material and money can be saved [67].

In conclusion, preventive maintenance can help to significantly increase the lifetime of a component and, in the production of cement to reduce its carbon footprint, it can be a way to help to reduce the emissions associated with it. With the added value of predictive maintenance, not only the lifetime will be extended but it will imply a saving of time and money and a reduction of waste of materials and, with it, extra help in reducing the carbon footprint and reaching the goal of the GCCA for 2050 of a Net Zero concrete.

7.3 Sustainable Development Goals

The Sustainable Development Goals are a list of 17 Goals adopted by all members of the United Nations in 2015 as part of the 2030 Agenda for Sustainable Development, a 15-year plan to achieve these goals, to end poverty, protect the planet and improve the lives and prospects of everyone, everywhere. Those goals include poor, rich and middle-income countries collaborating to promote prosperity while protecting the environment. They recognize that ending poverty must go hand-in-hand with strategies that build economic growth and address a range of social needs including education, health, social protection, and job opportunities while tackling climate change and environmental protection [68].

As can be observed in Figure 64, the 17 Sustainable Development Goals are the following:

Figure 64. Sustainable development goals (Source: Internet [68])

Each one of these goals is also divided into different sub-goals defined by more specific duties to achieve it.

In this chapter, a relationship between this thesis and Sustainable Development Goals will be performed to analyze which goals this thesis has an influence on and how it can have a positive impact on its achievement.

SDG		Goals		Influence on the thesis
Nº	Description	Nº	Description	
6	Clean water and sanitation	6.4	By 2030, substantially increase water-use efficiency across all sectors and ensure sustainable withdrawals and supply of freshwater to address water scarcity and substantially reduce the number of people suffering from water scarcity	The production of cement consumes almost a tenth of the industry's water [69]. By monitoring the state of the structures and performing maintenance exactly when needed the generation of unnecessary new cement and, due to that, the use of water can be reduced.
8	Economic growth	8.2	Achieve higher levels of economic productivity through diversification, technological upgrading, and innovation, including through a focus on high-value-added and labor-intensive sectors	Although it is not necessary, the implementation of a monitoring system is a value-added technological element that makes the structures more efficient.
9	Industry, innovation, and infrastructure	9.1	Develop quality, reliable, sustainable, and resilient infrastructure, including regional and transborder infrastructure, to support economic development and human well-being, with a focus on affordable and equitable access for all	A structure that has a DAQ system incorporated is monitored constantly, making it more reliable (failures can be predicted and prevented) and sustainable (maintenance will only be developed when needed, saving resources, and improving its lifetime). Additionally, in this thesis the DAQ system developed is a low-cost device, making it more affordable.
		9.4	By 2030, upgrade infrastructure and retrofit industries to make them sustainable, with increased resource-use efficiency and greater adoption of clean and environmentally sound technologies and industrial processes, with all countries taking action following their respective capabilities	Due to the maintenance of the structures will only be performed when needed, the use of resources will be more responsible.
		9.5	Enhance scientific research, upgrade the technological capabilities of industrial sectors in all countries, in particular	The DAQ systems that exist nowadays, as has been said, are expensive. This thesis is focused on developing a low-cost DAQ. This solution implies an

			developing countries, including, by 2030, encouraging innovation and substantially increasing the number of research and development workers per 1 million people and public and private research and development spending	innovation regards the existing DAQ systems.
11	Sustainable cities and communities	11.5	By 2030, significantly reduce the number of deaths and the number of people affected and substantially decrease the direct economic losses relative to the global gross domestic product caused by disasters, including water-related disasters, with a focus on protecting the poor and people in vulnerable situations	Applying a DAQ system to a structure is the first step to implementing predictive maintenance which will significantly reduce the chances of a building collapsing and damaging someone since it would be monitored, and the failures can be predicted and prevented.
12	Responsible consumption and production	12.2	By 2030, achieve the sustainable management and efficient use of natural resources	By performing the maintenance works only when needed, a significant number of resources can be saved
		12.5	By 2030, substantially reduce waste generation through prevention, reduction, recycling, and reuse	By extending the lifetime of a structure, the generation of waste is reduced.

Table 7. SDG covered by the thesis (Source: Own)

As can be observed, the development of a DAQ system for electromechanical testing and its applications have a significant impact on the pathway to a greener future, reducing the consumption of natural resources, the production of waste and extending the lifetime of any kind of structures, making them more reliable and safer.

8 Conclusions

This thesis had the aim of designing a low-cost DAQ system for electromechanical testing of smart materials. A set-up with an Arduino board as the main component and several peripherals to capture resistance and strain data was performed. It was installed in cement specimens and tested under cyclical loads. The extracted data was processed, and several conclusions could be extracted:

a) Electrical resistance and deformation are linearly related.
b) A higher gauge factor leads to a higher sensitivity to load detection.
c) Cement can be used as a strain sensor by itself, eliminating the need for strain gauges to detect the application of a load.
d) Discounting the human resources costs for development and testing, the replication of the designed DAQ system would be a low-cost solution for SHM, at least an order of magnitude more affordable than existing commercial solutions.

For future works, several options could be considered:

1. Test the functionality of the DAQ system on a cement reinforced with electrically conductive micro and nanofillers for improved piezoresistivity.
2. As has been said during the thesis, the strain gauge modules can only perform relative measures by themselves. For future work, it will be interesting to calibrate the modules with another sensor that could make absolute measurements.
3. Try to adapt the gain and data rate of the ADS1256 (since a higher gain and data speed also imply a higher noise) for being able to record data from the electrical current sensor.
4. Re-design the DAQ system for an AC power supply, potentially using the Arduino as a wave generator, and repeat the tests to obtain more accurate resistance values.
5. Expand the features of the designed DAQ system by notifying the user every time that a limit value of resistance is surpassed.
6. Improve the circuitry through soldered connections.

Overall, it can be considered that the DAQ system designed offers a low-price, full-functioning solution for monitoring the state of a self-sensing cement.

.

9 References

[1] ‘Qué es la programación con arduino y para qué sirve – Bejob’. https://www.bejob.com/que-es-la-programacion-con-arduino-y-para-que-sirve/ (accessed Jan. 28, 2023).

[2] ‘Truevolt Series 6.5 and 7.5 Digit Multimeters | Keysight’. https://www.keysight.com/us/en/products/digital-multimeters-dmm/truevolt-series-multimeters.html (accessed Jan. 28, 2023).

[3] ‘DMM6500 - Multímetro Digital, Banco, 15 Funciones, Pantalla Táctil 5", 10µA a 10A, 1ohm a 100MOhm, 6.5 Dígitos’. https://es.farnell.com/keithley/dmm6500/mult-metro-d-gitosal-banco-6-5/dp/2840447 (accessed Jan. 31, 2023).

[4] ‘Options and Upgrades: DAQ970A Data Acquisition System | Keysight’. https://www.keysight.com/us/en/options/DAQ970A/data-acquisition-system-usb-lan.html (accessed Feb. 3, 2023).

[5] ‘QuantumX Data Acquisition System | DAQ | Supplier | HBM’. https://www.hbm.com/en/2128/quantumx-compact-universal-data-acquisition-system/?product_type_no=QuantumX%20Data%20Acquisition%20System (accessed Feb. 3, 2023).

[6] ‘Sistemas CompactDAQ’. https://www.ni.com/es-es/shop/compactdaq.html (accessed Mar. 27, 2023).

[7] ‘Product’. https://www.ni.com/es-es/shop/hardware/products/compactdaq-chassis.html (accessed Mar. 27, 2023).

[8] ‘Módulo de Salida de Relé de la Serie C - NI’. https://www.ni.com/es-es/shop/hardware/products/c-series-relay-output-module.html (accessed Mar 27, 2023).

[9] ‘Product’. https://www.ni.com/es-es/shop/hardware/products/c-series-universal-analog-input-module.html (accessed Mar. 27, 2023).

[10] ‘Product’. https://www.ni.com/es-es/shop/hardware/products/compactdaq-controller.html (accessed Mar. 27, 2023).

[11] ‘Producto’. https://www.ni.com/es-es/shop/software/products/labview.html (accessed Mar. 29, 2023).

[12] A. Drougkas, V. Sarhosis, M. Basheer, A. D’Alessandro, and F. Ubertini, ‘Design of a smart lime mortar with conductive micro and nano fillers for structural health monitoring’, Construction and Building Materials, vol. 367, p. 130024, Feb. 2023, doi: 10.1016/j.conbuildmat.2022.130024.

[13] ‘Structural Health Monitoring’, HBM, Dec. 14, 2021. https://www.hbm.com/en/5530/structural-health-monitoring/?product_type_no=Structural%20Health%20Monitoring (accessed Mar. 6, 2023).

[14] J. M. Royo, '¿Qué es el SHM? Beneficios y Aplicaciones del Structural Health Monitoring', ITAINNOVA, Feb. 18, 2022. https://www.itainnova.es/blog/materiales/shm-beneficios-aplicaciones-structural-health-monitoring/ (accessed Feb. 18, 2023).

[15] 'Data Acquisition (DAQ) - The Ultimate Guide', Data Acquisition | Test and Measurement Solutions. https://dewesoft.com/blog/what-is-data-acquisition (accessed Mar. 27, 2023).

[16] 'Strain gauges for stress analysis & sensor production| Zemic Europe'. https://www.zemiceurope.com/en/products/strain-gauges.html (accessed Mar. 23, 2023).

[17] 'Medir tensión con galgas extensiométricas'. https://www.ni.com/es-es/shop/data-acquisition/sensor-fundamentals/measuring-strain-with-strain-gages.html (accessed Mar. 23, 2023).

[18] 'Vibrating Wire Strain Gauge', RST Instruments Ltd. https://rstinstruments.com/product/vibrating-wire-strain-gauge/ (accessed Mar. 23, 2023).

[19] 'Monitoreo de Salud Estructural', Soluciones de Adquisición de Datos (DAQ). https://dewesoft.com/es/aplicaciones/monitoreo-de-salud-estructural (accessed Mar. 23, 2023).

[20] 'vibrating wire strain gauge, vibrating wire strain gauge Suppliers and Manufacturers at Alibaba.com'. https://www.alibaba.com/showroom/vibrating-wire-strain-gauge.html (accessed Mar. 23, 2023).

[21] 'LB11/TB21 Strain Gauges for Measuring in Screws & Bolts', HBM, Nov. 24, 2021. https://www.hbm.com/en/7452/cylindric-strain-gauges-for-measurements-in-bolts/?product_type_no=LB11/TB21%20Strain%20Gauges%20for%20Measuring%20in%20Screws%20&%20Bolts (accessed Mar. 23, 2023).

[22] 'Bolt Strain Gauge | Tokyo Measuring Instruments Laboratory Co., Ltd.' https://tml.jp/e/product/strain_gauge/btm_list.html (accessed Mar. 23, 2023).

[23] 'Strain Gauges for Determination of Residual Stress', HBM, Nov. 12, 2021. https://www.hbm.com/en/3454/strain-gauges-for-residual-stress-measurements/?product_type_no=Strain%20Gauges%20for%20Determination%20of%20Residual%20Stress (accessed Mar. 23, 2023).

[24] 'Residual Stress Strain Gauges'. https://es.omega.com/pptst/SGD_StressRelief.html (accessed Mar. 23, 2023).

[25] 'Nuevas tecnologías para pruebas estructurales y monitoreo de condición'. https://www.ni.com/es-es/shop/compactrio/new-technologies-for-structural-testing-and-health-monitoring.html (accessed Mar. 27, 2023).

[26] 'Cómo escoger el hardware DAQ adecuado para su sistema de medidas'. https://www.ni.com/es-es/shop/data-acquisition/how-to-choose-the-right-daq-hardware-for-your-measurement-system.html (accessed Mar. 27, 2023).

[27] J. J. Villacorta et al., 'Design and Validation of a Scalable, Reconfigurable and Low-Cost Structural Health Monitoring System', Sensors, vol. 21, no. 2, p. 648, Jan. 2021, doi: 10.3390/s21020648.

[28] S. Komarizadehasl, B. Mobaraki, H. Ma, J.-A. Lozano-Galant, and J. Turmo, 'Development of a Low-Cost System for the Accurate Measurement of Structural Vibrations', Sensors, vol. 21, no. 18, p. 6191, Jan. 2021, doi: 10.3390/s21186191.

[29] H. Louw, A. Broekman, and E. Kearsley, 'MADV-DAQ: Multi-channel Arduino-based differential voltage data acquisition system for remote strain measurement applications', HardwareX, vol. 12, p. e00360, Oct. 2022, doi: 10.1016/j.ohx.2022.e00360.

[30] A. L. Silva, M. Varanis, A. G. Mereles, C. Oliveira, and J. M. Balthazar, 'A study of strain and deformation measurement using the Arduino microcontroller and strain gauges devices', Rev. Bras. Ensino Fís., vol. 41, Dec. 2018, doi: 10.1590/1806-9126-RBEF-2018-0206.

[32] P. T. Dalla, K. G. Dassios, I. K. Tragazikis, D. A. Exarchos, and T. E. Matikas, 'Carbon nanotubes and nanofibers as strain and damage sensors for smart cement', Materials Today Communications, vol. 8, pp. 196–204, Sep. 2016, doi: 10.1016/j.mtcomm.2016.07.004.

[33] S. Ding et al., 'In-situ synthesizing carbon nanotubes on cement to develop self-sensing cementitious composites for smart high-speed rail infrastructures', Nano Today, vol. 43, p. 101438, Apr. 2022, doi: 10.1016/j.nantod.2022.101438.

[34] W. Dong et al., 'Application of intrinsic self-sensing cement-based sensor for traffic detection of human motion and vehicle speed', Construction and Building Materials, vol. 355, p. 129130, Nov. 2022, doi: 10.1016/j.conbuildmat.2022.129130.

[35] 'Different Parts of Arduino Uno Board', STEMpedia Learning Center. https://learn.thestempedia.com/courses/introductory-course-on-arduino/lessons/getting-started-5/topic/different-parts-of-arduino-board/ (accessed Feb. 7, 2023).

[36] 'Arduino - Home'. https://www.arduino.cc/ (accessed Feb. 8, 2023).

[37] T. Nachazel, 'What is a Strain Gauge and How Does it Work?', Michigan Scientific Corporation, Aug. 13, 2020. https://www.michsci.com/what-is-a-strain-gauge/ (accessed Feb. 8, 2023).

[38] 'Strain Gauge: Working Principle & Diagram | Electrical4U', https://www.electrical4u.com/, Oct. 22, 2020. https://www.electrical4u.com/strain-gauge/ (accessed Feb. 8, 2023).

[39] 'BF350-3AA Strain Gauge Module', Hobby Components. https://hobbycomponents.com/sensors/963-bf350-3aa-strain-gauge-module (accessed Feb. 8, 2023).

[40] 'Crowtail- Strain Gauge Sensor (ER-CT0070SGS)', RLX COMPONENTS s.r.o. Electronic Components Distributor. https://rlx.sk/en/breakout-boards-shields/5564-crowtail-strain-gauge-sensor-er-ct0070sgs.html (accessed Feb. 8, 2023).

[41] 'Strain Gauge Module (ER-SEN77631Y3) BF350-3AA extenzometer/tenzometer', RLX COMPONENTS s.r.o. Electronic Components Distributor. https://rlx.sk/en/measurement-boards/4446-strain-gauge-module-er-sen77631y3-bf350-3aa.html (accessed Feb. 08, 2023).

[42]'ADS1256 pdf, ADS1256 Descripción Electrónicos, ADS1256 Datasheet, ADS1256 view ::: ALLDATASHEET ': https://pdf1.alldatasheet.es/datasheet-pdf/view/336384/TI/ADS1256.html (accessed Jun. 03, 2023).

[43]'DollaTek ADS1256 24bit 8channel ADC AD módulo de Alta precisión ADC módulo de adquisición de Datos de adquisición : Amazon.es: Electrónica'. https://www.amazon.es/DollaTek-ADS1256-8channel-precisi%C3%B3n-adquisici%C3%B3n/dp/B07DK5GC9H/ref=sr_1_3?__mk_es_ES=%C3%85M%C3%85%C5%BD%C3%95%C3%91&crid=PAUHFK0W3CC&keywords=ADS1256&qid=1676974735&s=electronics&sprefix=ads1256%2Celectronics%2C94&sr=1-3 (accessed Jun. 08, 2023).

[43] S. Projects, 'Electric Current Measurement Using Arduino and ACS758 Sensor', SIMPLE PROJECTS, Aug. 17, 2021. https://simple-circuit.com/interface-arduino-allegro-acs758-current-sensor-ac-dc/ (accessed Feb. 24, 2023).

[45] R. Lozano, '¿Como medir corriente con sensor INA219 arduino?', Talos Electronics, Nov. 21, 2021. https://www.taloselectronics.com/blogs/tutoriales/como-medir-corriente-con-sensor-ina219-arduino (accessed Feb. 24, 2023).

[46] 'Medir intensidad y consumo eléctrico con Arduino y ACS712', Luis Llamas, Jan. 18, 2017. https://www.luisllamas.es/arduino-intensidad-consumo-electrico-acs712/ (accessed Feb. 24, 2023).

[47] 'Tutorial sensor de corriente ACS712', Naylamp Mechatronics - Perú. https://naylampmechatronics.com/blog/48_tutorial-sensor-de-corriente-acs712.html (accessed Jun. 10, 2023).

[48] 'Voltage divider', Wikipedia. Mar. 31, 2023. Accessed: Jun. 08, 2023. [Online]. Available: https://en.wikipedia.org/w/index.php?title=Voltage_divider&oldid=1147585673

[49] M. Bilsky, ADS1256-and-Arduino. 2023. Accessed: Jun. 03, 2023. [Online]. Available: https://github.com/mbilsky/ADS1256-and-Arduino

[50] ADS1xxx-Series-ADC-Libraries/ADS1255-ADS1256. ADS1xxx- Series ADC Libraries, 2023. Accessed: Jun. 03, 2023. [Online]. Available: https://github.com/ADS1xxx-Series-ADC-Libraries/ADS1255-ADS1256

[51] Matt Bilsky, Connecting an ADS1256 to the Arduino UNO and MEGA, (Jul. 10, 2019). Accessed: Jun. 03, 2023. [Online Video]. Available: https://www.youtube.com/watch?v=xZ4ib39RXb0

[52] 'How to Make an Arduino Ohm Meter'. https://www.circuitbasics.com/arduino-ohm-meter/ (accessed Jun. 03, 2023).

[53] 'Strain Gauge Module'. https://www.elecrow.com/strain-gauge-module-p-735.html (accessed Jun. 10, 2023).

[54] 'What's a Strain Gage | KYOWA'. https://www.kyowa-ei.com/eng/technical/strain-basic_course/index.html (accessed Jun. 10, 2023).

[55] G. Hollings, 'Strain Gauges: How they Work, Applications, and Types'. https://blog.endaq.com/strain-gauges-how-they-work-applications-and-types (accessed Jun. 10, 2023).

[56] 'Dieléctrico', Wikipedia, la enciclopedia libre. May 27, 2023. Accessed: Jun. 11, 2023. [Online]. Available: https://es.wikipedia.org/w/index.php?title=Diel%C3%A9ctrico&oldid=151465633

[57] M. Tamov, V. Pochinok, G. R. Tabagua, and M. Tamov, 'Elimination of polarization effect in DC measurement of resistivity of CNT-cement composites', IOP Conf. Ser.: Mater. Sci. Eng., vol. 869, no. 5, p. 052060, Jun. 2020, doi: 10.1088/1757-899X/869/5/052060.

[58] S. Mundo, 'El cemento contamina más que todos los camiones del mundo', Sputnik Mundo. https://sputniknews.lat/20190624/cemento-contaminacion-co2-cliker-alternativas-1087752102.html (accessed Feb. 22, 2023).

[59] S. Romero, '¿Puede la industria del hormigón realmente volverse neutra en carbono para 2050?', elconfidencial.com, Jan. 04, 2022. https://www.elconfidencial.com/medioambiente/ciudad/2022-01-04/cemento-hormigon-emisiones-co2-sostenible_3098260/ (accessed Feb. 21, 2023).

[60]Á. Hermida, 'Cemento y crísis climática: cómo el material supremo calienta el planeta', elconfidencial.com, Feb. 15, 2021. https://www.elconfidencial.com/medioambiente/ciudad/2021-02-15/cemento-gases-efecto-invernadero-calentamiento_2944723/ (accessed Feb. 21, 2023).

[61] 'La enorme fuente de emisiones de CO2 que está por todas partes y que quizás no conocías', BBC News Mundo. Accessed: Feb. 21, 2023. [Online]. Available: https://www.bbc.com/mundo/noticias-46594783

[62] 'Actions to a net zero future', GCCS | Staging. https://gccassociation.org/concretefuture/actions-to-a-net-zero-future/ (accessed Feb. 22, 2023).

[63] J. Li, G. Yin, X. Wang, and W. Yan, 'Automated decision making in highway pavement preventive maintenance based on deep learning', Automation in Construction, vol. 135, p. 104111, Mar. 2022, doi: 10.1016/j.autcon.2021.104111.

[64] 'What Is Preventive Maintenance? The Complete Guide To PM | Fiix'. https://www.fiixsoftware.com/maintenance-strategies/preventative-maintenance/ (accessed Feb. 20, 2023).

[65] 'What is Predictive Maintenance?', TIBCO Software. https://www.tibco.com/reference-center/what-is-predictive-maintenance (accessed Feb. 20, 2023).

[66] 'What is Preventive Maintenance? Types, Examples and Benefits | IBM'. https://www.ibm.com/topics/what-is-preventive-maintenance (accessed Feb. 22, 2023).

[67] B. Taşcı, A. Omar, and S. Ayvaz, 'Remaining Useful Lifetime Prediction for Predictive Maintenance in Manufacturing'. Rochester, NY, Jan. 31, 2023. doi: 10.2139/ssrn.4344017.

[68] 'THE 17 GOALS | Sustainable Development'. https://sdgs.un.org/es/goals (accessed Feb. 23, 2023).

[69] J. Watts, 'Cemento: el material más destructivo de la Tierra', elDiario.es, Mar. 04, 2019. https://www.eldiario.es/internacional/theguardian/cemento-material-destructivo-tierra_1_1675968.html (accessed Feb. 23, 2023).